TECHNISCHE UNIVERSITÄT WIEN
Vienna University of Technology

Operations Research and Control Systems

Numerical computation of the optimal vector field: exemplified by a fishery model

Dieter Grass

Research Report 2012-12

December 2012

Operations Research and Control Systems
Institute of Mathematical Methods in Economics
Vienna University of Technology

Research Unit ORCOS
Argentinierstraße 8/E105-4,
1040 Vienna, Austria
E-mail: orcos@eos.tuwien.ac.at

Numerical computation of the optimal vector field: exemplified by a fishery model

D. Graß*

Abstract

Numerous of the optimal control models analyzed in economics are formulated as discounted infinite time horizon problems, where the defining functions are nonlinear as well in the states as in the controls. As a consequence solutions can often only be found numerically. Moreover, the long run optimal solutions are mostly limit sets like equilibria or limit cycles. Using these specific solutions a BVP approach together with a continuation technique is used to calculate the parameter dependent dynamic structure of the optimal vector field. We use a one dimensional optimal control model of a fishery to exemplify the numerical techniques. But these methods are applicable to a much wider class of optimal control problems with a moderate number of state and control variables.

1 Introduction

During the last decades optimal control models have successfully been applied in economics and ecology. Many of these models exhibit non-concavities and depend on multiple parameters. As a consequence analytical methods alone are often insufficient for a full analysis. These nonlinearities often also give rise to the occurrence of multiple or history-dependent solutions. Therefore a well adapted numerical framework is needed, allowing an efficient handling of qualitatively different solutions.

The occurring phenomena are various. These range from history-dependence, i.e. dependent on the initial value one converges to different attractors, to multiplicity, where for specific points the decision maker is indifferent choosing between different optimal solutions. This multitude of solution behavior, corresponding to non-uniqueness or existence of different long run attractors, is scattered over a wide variety of articles, where a few of them are mentioned below. For a survey of literature on this field the reader is referred to Grass et al. (16, Ch. 5).

*ORCOS, Institute of Mathematical Methods in Economics, Vienna University of Technology, A-1040 Vienna, Austria. E-mail: dieter.grass@tuwien.ac.at

The literature at this point lacks a theoretical and well structured description of these different phenomena, which correspond to structural changes in the optimal solution. Thus they can be further ascribed as bifurcations of the optimal vector field. Developing a comprehensive bifurcation theory of the optimal vector field is however done in Kiseleva and Wagener (22) and Kiseleva (21) for the one dimensional shallow lake model. But a bifurcation theory of the optimal vector field for two and higher dimensional systems is still missing.

Some remarks regarding the notation, classifying the phenomena of multiplicity and/or dependence on the initial values, should however be given. We already mentioned that in this context not only a theoretical framework is missing, also a standardized notation is lacking. For points exhibiting multiple optimal solutions an often used term is that of a Skiba point, or as introduced by myself in Grass et al. (16) DNSS point, recognizing the individual contributions of the authors Dechert, Nishimura, Skiba, and Sethi. But to avoid a discussion of first priority we adopt to the terminology of indifference points/thresholds that was introduced in Kiseleva and Wagener (22) and Kiseleva (21). Even though this terminology has also been criticized it turns out advantageous compared to unnecessarily long and complicated acronyms.

Bifurcations of the optimal vector field often correspond to global bifurcations of the canonical system derived from the underlying optimal control problem, (see, e.g., 31, 32), therefore efficient numerical tools are necessary for the calculations. Also the use of high-level illustrations and animations are of great help for the development of a bifurcation theory. These visualizations provide the necessary intuition for the facts which then have to be proved rigorously. The aim of this article is the introduction to a numerical approach specifically well adapted to infinite time horizon problems. For this approach information of the possible behavior of the solution at infinite is used to formulate a BVP. To solve the hence resulting BVP a continuation (homotopy) technique is used. A preliminary version of these numerical tools is implemented as a MATLAB package `OCMat`, which can be downloaded at `http://orcos.tuwien.ac.at/research/ocmat_software`. At this website the interested reader can also find slides of an introductory seminar about the toolbox.

To exemplify these numerical techniques we use a one state, one control fishery model. This model is a simplified version of a three state optimal control problem, formulated in Crépin (9). But these numerical techniques can in principle be applied to models with an arbitrary number of states, controls and constraints. The limitations of this method are more of practical nature, e.g. computational capacity, than theoretical nature. In fact the MATLAB package `OCMat` has already been successfully applied to a number of different models, e.g., (3, 5, 4, 6, 8, 7, 34, 27). The presented bifurcations have analogous counterparts in higher dimensions and can numerically be computed using the same procedures. More complex bifurcations can occur when the number of states increase, e.g. an equilibrium can be replaced by a limit cycle. For obvious reasons these bifurcations cannot be found in the one dimensional case. These bifurcations are the topic of ongoing research and will be presented in future

articles.

Before we start with the presentation of the general problem formulation and the numerical techniques for its numerical analysis let me clarify a few points. The fishery model is only used as a vehicle supporting the reader, who is unfamiliar with the numerical method, to adapt and apply it for her/his own models. It is not my intention to interpret the results from an economic point of view. This will be done on a different place.

Even though the examples for the numerical techniques are stated only for a one state, one control and one constraint model in most cases the algorithm can immediately be adapted to higher dimensional problems. Therefore, in the main cases I added a subsection where the underlying BVP of the specific fishery model is also formulated for the general model in higher dimensions.

To interpret the numerical results in a correct way the assumptions, like existence of an optimal solution and convergence of the optimal path to an equilibrium have to be proved separately. For the fishery model these assumptions are proved in A. In general this should be part of the analysis and is independent from the numerical calculations, which otherwise only yield candidates for an optimal solution.

Subsequently we present a numerical technique for analyzing discounted problems over an infinite time horizon of the following type

$$\max_{u(\cdot)} \int_0^\infty \mathrm{e}^{-rt}\, g(x(t), u(t), \mu)\ \mathrm{d}t \tag{1a}$$

$$\text{s.t.} \quad \dot{x}(t) = f(x(t), u(t), \mu), \quad t \in [0,\, \infty) \tag{1b}$$

$$\text{with} \quad x(0) = x_0 \tag{1c}$$

$$k(x(t), u(t), \mu) \geq 0, \quad t \in [0,\, \infty). \tag{1d}$$

with $x(t) \in \mathbb{R}^n$, $u(t) \in \mathbb{R}^m$ and the state dynamics $f : \mathbb{R}^{n+m} \to \mathbb{R}^n$, the objective function $g : \mathbb{R}^{n+m} \to \mathbb{R}$, and the mixed path constraints $k : \mathbb{R}^{n+m} \to \mathbb{R}^l$, are assumed to be two times continuously differentiable in their arguments. Additionally, the functions may depend on some parameter values $\mu \in \mathbb{R}^k$. To simplify notation we omit this explicit dependence on parameter values wherever this dependence on parameter values is not crucial for the computations.

Next we formulate assumptions which have to be checked analytically for a concrete model, or if an exact proof is not possible one has to be aware that solutions which satisfy the necessary optimality conditions are only extremals, i.e., candidates for optimal solutions.

Assumptions 1.

a) There exists an optimal solution $(x^*(\cdot), u^*(\cdot))$ for every $x_0 \in C \subset \mathbb{R}^n$, with C a compact set.

b) The constraints (1d) satisfy the constraint qualification

$$k_u(x, u, \mu) \neq 0 \tag{2}$$

for every $x \in \mathbb{R}^n$ and $u \in \mathbb{R}^m$.

We postulate the existence of an optimal solution instead of formulating conditions, which guarantee the existence. This reflects the fact that for many models these general conditions are not satisfied. Therefore showing the existence of an optimal solution is a separate task.

Furthermore we state assumptions which could be made less restrictive, but simplify the following presentation

Assumptions 2.

a) The control variable u appears nonlinearly either in the function $g(x, u, \mu)$ or in the function $f(x, u, \mu)$.

b) The Hamiltonian maximizing condition can be solved analytically.

c) Every optimal solution $(x^*(\cdot), u^*(\cdot))$ converges to an equilibrium.[1]

Definition 1. Let $(x^*(\cdot), u^*(\cdot))$ be a solution of problem (1) converging to the equilibrium $(\hat{x}, \hat{u})$ then the equilibrium is called the *long run optimal solution*. An optimal solution $(x^*(\cdot), u^*(\cdot))$ of problem (1) with initial condition $x(0) = \hat{x}$ and $(x^*(t), u^*(t)) = (\hat{x}, \hat{u})$ for all $t \geq 0$ is called an *equilibrium solution*.

The right hand side of the ODEs (1b), where the control $u(\cdot)$ is replaced by the optimal control $u^*(\cdot)$, i.e.

$$\dot{x}(t) = f(x(t), u^*(t), \mu) \tag{3}$$

is called the *optimal vector field* of problem (1).

Remark 1. For autonomous infinite time horizon problems the assumption that the solution converges to an equilibrium (or in higher dimensions to a limit cycle) is not very restrictive. In fact for nearly every model the author analyzed the last years this assumption was satisfied. Moreover, since for discounted problems stable equilibria, of the canonical system, are ruled out, saddle-points are the first candidates for long run optimal solutions. Anyhow, the reader has to be aware that the assumption that the solution converges to an equilibrium (limit cycle) restricts the number of possible candidates and if e.g. diverging optimal paths cannot be excluded the algorithms have to be adapted to handle such a situation. Since these adaptations are very model specific we will not go into any details.

1.1 Necessary optimality conditions

For a profound introduction into the theory of optimal control problems the reader is referred to Seierstad and Sydsaeter (30), Kamien and Schwartz (20), for a more applicational oriented approach to Grass et al. (16) or any other of the numerous text books on this topic. Let

$$\mathcal{H}(x, u, \lambda, \lambda_0, \mu) := \lambda_0 g(x, u, \mu) + \lambda f(x, u, \mu) \tag{4}$$

[1]Throughout this paper an equilibrium is always understood in the sense of dynamical systems, i.e., as a point where the dynamics is zero.

be the Hamiltonian function and

$$\mathcal{L}(x, u, \lambda, \lambda_0, \mu, \psi) := \mathcal{H}(x, u, \lambda, \lambda_0, \mu) + \psi k(x, u, \mu) \tag{5}$$

the Lagrangian function. Then, under the given Assumption 1 and Assumption 2 an optimal solution $(x^*(\cdot), u^*(\cdot))$ of (1) has to satisfy the Hamiltonian maximizing condition

$$u^*(t) = \underset{u \in \mathbb{R}^m}{\operatorname{argmax}} \mathcal{H}(x^*(t), u, \lambda(t), \lambda_0, \mu), \quad \text{with} \quad k(x^*(t), u, \mu) \geq 0. \tag{6}$$

The Lagrangian multiplier $\psi(\cdot)$ has to satisfy the complementary slackness and positivity conditions

$$\psi(t)k(x^*(t), u^*(t), \mu) = 0 \quad \text{and} \quad \psi(t) \geq 0.$$

Finally the costate $\lambda(\cdot)$ satisfies the adjoint system

$$\dot{\lambda}(t) = r\lambda(t) - \frac{\partial \mathcal{L}}{\partial x}(x^*(t), u^*(t), \lambda(t), \lambda_0, \mu, \psi(t))$$

which together with the state dynamics

$$\dot{x}^*(t) = f(x^*(t), u^*(t))$$

is called the canonical system.

We often make use of the identity, cf. Michel (28)

$$\frac{1}{r}\mathcal{H}(x(0), u(0), \lambda(0), \mu) = \int_0^\infty \mathrm{e}^{-rt}\, g(x(t), u(t), \mu)\ \mathrm{d}t, \tag{8}$$

where $(x(\cdot), u(\cdot), \lambda(\cdot))$ satisfies the necessary optimality conditions, but is not necessarily an optimal solution. This identity allows us to compare the objective values of two candidate solutions by actually comparing their Hamiltonian values. Due to the time invariance of autonomous problems (8) holds true for every point of a solution path, and not only at the initial point.

In the subsequent sections we use a specific model, which is of this general type (1). We structured the paper in a way that the used numerical algorithms are firstly formulated and applied to this specific model and then stated for the general problem. We hope that this ease the understanding of the numerics and enable the reader to apply this numerical approach to more involved problems.

2 A fishery model

The full fishery model in a coral reef presented in Crépin (9) consists, at time t, of the three states fish $x(t)$, algae $a(t)$, coral $c(t)$, and the control $u(t)$ representing the effort of fishing. In our simplified version we will set the number of algae and coral constant, i.e, $a(\cdot) \equiv a$ and $c(\cdot) \equiv c$, yielding a one state, one control optimal control problem.

The dynamics of fish is described by a logistic growth term G, with a carrying capacity depending linearly on the number of algae, yielding

$$G(t) := x(t)\left(1 - \frac{x(t)}{a}\right).$$

Additionally we have a term stemming from predation P which is decreasing with the number of corals, because of coral giving shelter to the fish. This term can be modeled by

$$P(t) := \frac{1}{(c+\tau)}\frac{x(t)^2}{1+x(t)^2}.$$

The stock of fish is also reduced by fishing $u(t)x(t)$, yielding the total fish dynamics as

$$\begin{aligned}\dot{x}(t) &= G(t) - P(t) - u(t)x(t)\\ &= x(t)\left(1 - \frac{x(t)}{a}\right) - \frac{1}{(c+\tau)}\frac{x(t)^2}{1+x(t)^2} - u(t)x(t).\end{aligned}$$

To formulate the economic part of the model we simply assume that fishing yields positive gains from selling them at price p but also generates negative (ecological) side effects. Thus, we define the total instantaneous utility as

$$U(t) := pu(t)x(t) - u(t)^2.$$

Summing up, the optimal control problem can be written as

$$\max_{u(\cdot)} \left\{ \int_0^\infty \mathrm{e}^{-rt}\left(pu(t)x(t) - u(t)^2\right)\mathrm{d}t \right\} \tag{9a}$$

$$\text{s.t.} \quad \dot{x}(t) = x(t)\left(1 - \frac{x(t)}{a}\right) - \frac{1}{(c+\tau)}\frac{x(t)^2}{1+x(t)^2} - u(t)x(t) \tag{9b}$$

$$u(t) \geq 0, \quad \text{for all} \quad t \tag{9c}$$

$$x(0) = x_0 > 0. \tag{9d}$$

For the analysis of this model Pontryagin's Maximum Principle is used, where the details are carried out in the next section.

2.1 Necessary optimality conditions

Defining the Hamiltonian and Lagrangian (augmented Hamiltonian) of problem (9) as

$$\mathcal{H}(x,u,\lambda,\lambda_0) := \lambda_0\left(pux - u^2\right) + \lambda\left(x\left(1 - \frac{x}{a}\right) - \frac{1}{(c+\tau)}\frac{x^2}{1+x^2} - ux\right) \tag{10}$$

$$\mathcal{L}(x,u,\lambda,\psi,\lambda_0) := \mathcal{H}(x,u,\lambda,\lambda_0) + \psi u \tag{11}$$

an optimal solution $(x^*(\cdot), u^*(\cdot))$ of (9) has to satisfy the following necessary optimality conditions. There exists a (piecewise) continuous function $\psi(\cdot)$ and

a (piecewise) differentiable function $\lambda(\cdot)$ with $(\lambda(t), \lambda_0) \neq (0,0),\ t \geq 0$, such that at every time point t

$$u^*(t) \in \underset{u \geq 0}{\operatorname{argmax}}\, \mathcal{H}(x^*(t), u(t), \lambda(t), \lambda_0) \tag{12}$$

and

$$\dot{\lambda}(t) = r\lambda(t) - \frac{\partial \mathcal{L}}{\partial x}(x^*(t), u^*(t), \lambda(t), \psi(t), \lambda_0) \tag{13}$$

with the transversality condition

$$\lim_{t \to \infty} \mathrm{e}^{-rt}\, \lambda(t) = 0. \tag{14}$$

In App. A.1 it is proved that the problem (9) is normal, i.e. $\lambda_0 > 0$, and therefore λ_0 can be set to one and is subsequently omitted.[2] Since the Hamiltonian (10) is strictly concave with respect to u the Hamiltonian maximizing condition (12) can be reformulated as

$$\frac{\partial \mathcal{L}}{\partial u}(x^*(t), u^*(t), \lambda(t), \psi(t)) = 0 \tag{15a}$$

$$\psi(t) \geq 0 \tag{15b}$$

$$\psi(t) u^*(t) = 0. \tag{15c}$$

From (15a) we find that the maximizer

$$u^\circ = \underset{u \geq 0}{\operatorname{argmax}}\, \mathcal{H}(x, u, \lambda) \tag{16}$$

can be derived from

$$\frac{\partial \mathcal{H}}{\partial u} = px - 2u - \lambda x = 0 \Leftrightarrow u = u^\bullet := \frac{x}{2}(p - \lambda)$$
$$\frac{\partial \mathcal{L}}{\partial u} = px - 2u - \lambda x + \psi = 0,$$

where $u^\bullet$ is the unconstrained maximizer. Using (15b) and (15c) finally yields

$$u^\circ = \begin{cases} u^\bullet & \text{for} \quad \lambda \leq p \\ 0 & \text{for} \quad \lambda \geq p \end{cases} \tag{17}$$

$$\psi = \begin{cases} 0 & \text{for} \quad \lambda \leq p \\ -x(p - \lambda) & \text{for} \quad \lambda \geq p. \end{cases} \tag{18}$$

In App. A.2 the continuity of the optimal control $u^*(\cdot)$ and the Lagrangian multiplier $\psi(\cdot)$ is proved. Not to confuse the reader, u° (and $u^\circ(t)$) denote the analytical term for the control value (at time t) after solving the (static)

[2] A well known example showing that infinite time horizon problem need not be normal can be found in Halkin (17).

maximization (16) at time t, whereas $u^*(\cdot)$ denotes the searched for optimal control.

Summing up an optimal solution $(x^*(\cdot), u^*(\cdot))$ for the problem (9) has to be searched among the solutions $(x(\cdot), u^\circ(\cdot), \lambda(\cdot))$ of the so called canonical system given by

$$\dot{x}(t) = x(t)\left(1 - \frac{x(t)}{a}\right) - \frac{1}{(c+\tau)}\frac{x(t)^2}{1+x(t)^2} - u^\circ(t)x(t) \tag{19a}$$

$$\dot{\lambda}(t) = \lambda(t)\left(r - 1 + \frac{2x(t)}{a} + \frac{2x(t)}{(c+\tau)(1+x(t)^2)^2}\right) - u^\circ(t)(p - \lambda(t)) \tag{19b}$$

satisfying the boundary conditions

$$x(0) = x_0 \quad \text{and} \quad \lim_{t\to\infty} \mathrm{e}^{-rt}\,\lambda(t) = 0.$$

From a numerical point of view the transversality condition (14) does not provide information to explicitly calculate solutions of the system (19a) and (19b). But paths $(x(\cdot), \lambda(\cdot))$ converging to an equilibrium $(\hat{x}, \hat{\lambda})$ trivially satisfy the transversality condition (14) and therefore are possible solution candidates.[3] For the model (9) it is proved in App. A.3 that the stable paths, which are solutions converging to an equilibrium, are already all candidates for the optimal solution.

Thus we restated the problem of finding candidates for optimal paths, as a problem of finding the equilibria $(\hat{x}, \hat{\lambda})$ of the ODEs (19a) and (19b), and calculating the corresponding stable paths. In case of multiple equilibria and multiple solutions we have to compare the corresponding value of the objective function and choose the maximizer.

3 Calculating stable paths

The core step of the here presented algorithm is the calculation of a stable path within a BVP framework using a continuation (homotopy) strategy. The calculation of a stable path is of course not restricted to optimal control problems and we will therefore present this algorithm in a more general setting of an ODE

$$\dot{y}(t) = g(y(t), \mu), \quad y = (y^1, y^2)' \in \mathbb{R}^{n_s \times n_u}, \quad n_s + n_u = n \tag{20a}$$

depending on parameter values $\mu \in \mathbb{R}^k$, or even shorter

$$\dot{y}(t) = g(y(t)), \tag{20b}$$

whenever the parameter values μ are constant during the calculations. For notational clarity, the symbol $(\cdot)'$ denotes matrix/vector transposition throughout the paper.

[3] The transversality condition for infinite time horizon problems is a topic for its own and will not further be discussed at this point. It is also of minor importance since the here presented numerical procedure are done under the assumption that the solution converges to an equilibrium. The verification of this assumption has to be given separately.

We assume that the system (20) exhibits a hyperbolic saddle point $\hat{y}$, with an n_s dimensional stable and an n_u dimensional unstable (local) manifold. The eigenvalues $\xi_i^s,\ i = 1, \ldots, n_s$ and $\xi_i^u,\ i = 1, \ldots, n_u$ of the Jacobian matrix

$$J(\hat{y}) := \frac{\partial}{\partial y} g(y) \mid_{y=\hat{y}}$$

satisfy $\mathrm{Re}\, \xi_i^s < 0 < \mathrm{Re}\, \xi_j^u$.

The problem is to find, for a given initial state $y_0^1 \in \mathbb{R}^{n_s}$, a solution path $y(\cdot)$ of (20) satisfying

$$y^1(0) = y_0^1 \tag{21}$$

and

$$\lim_{t \to \infty} y(t) = \hat{y}. \tag{22}$$

In the terminology of App. B this determines a (two-point) boundary value problem (TBVP), with $T = \infty$. To solve this problem numerically we have to reformulate the asymptotic condition (22), translating the convergence property into some "finite" setting.

A solution path $y(\cdot)$ satisfying (22) lies in the global stable manifold of $\hat{y}$ and reaches therefore the local stable manifold in some finite time (cf. (61)).

The manifold theorem (see App. B, Th. 1) states that the local stable manifold at $\hat{y}$ is tangent to the stable eigenspace $\mathrm{E}^s(\hat{y})$. For reasons of simplicity we assume that the eigenvectors build a basis of $\mathbb{R}^n$ (otherwise generalized eigenvectors have to be considered), then the stable eigenspace is given by

$$\mathrm{E}^s(\hat{y}) = \sum_{i=1}^{n_s} \kappa_i \nu_i^s \in \mathbb{R}^n,\ \kappa_i \in \mathbb{R} \tag{23}$$

with ν_i^s being the eigenvector corresponding to the eigenvalue ξ_i^s. Thus, the condition (22) can approximately be replaced by

$$(y(T) - \hat{y}) \in \mathrm{E}^s(\hat{y}), \tag{24}$$

for T large enough. Moreover, the condition (24) is equivalent to the equation

$$F'(y(T) - \hat{y}) = 0, \tag{25}$$

where the matrix $F \in \mathbb{R}^{n_u \times n}$ is given by a basis spanning the orthogonal complement to the stable eigenspace. Its actual computation is described in Th. 2 of App. B and simplifies for the one dimensional case to $F := (\nu_1^s)^\perp$. The theoretical justification for condition (25) as an approximation of (22) can be found e.g. in de Hoog and Weiss (10) and Palmer (29).

3.1 The boundary value problem

Summing up, the problem of finding a stable path satisfying (22) can (approximatively) be calculated by solving (25). Additionally, we normalize the time

interval $[0, T]$ to $[0, 1]$ (see B.1). Therefore, a solution $y(\cdot)$ starting at y_0^1 and converging to $\hat{y}$ can numerically be computed by fixing end time T (large enough) and solving the BVP

$$\dot{y}(t) = Tg(y(t)),\ t \in [0, 1] \tag{26a}$$
$$y^1(0) = y_0^1 \in \mathbb{R}^{n_s} \tag{26b}$$
$$F'(y(1) - \hat{y}) = 0 \in \mathbb{R}^{n_u}, \tag{26c}$$

where (26c) is called the *asymptotic transversality condition*. The appearance of T in (26a) is due to the normalization of the time interval. The BVP (26) is correctly stated since the number of unknowns n equals that of the boundary conditions $n_s + n_u = n$ and the boundary conditions are linearly independent.

Remark 2 (Unstable path). An unstable path can be calculated in an analogous way by reversing the direction of time, i.e., replacing the dynamics (26a) by

$$\dot{y}(t) = -Tg(y(t)),\ t \in [0, 1],$$

and the matrix F in (26c) has to be calculated for the unstable eigenspace.

Remark 3. The advantage of truncating the time interval to a fixed value is the linearity of the boundary condition (26c). But the apparent drawback is the principle indefiniteness in choosing the truncation time T. Thus, one has to take care that during the computations the chosen time T is large enough, i.e, the distance $\|y(T) - \hat{y}\|$ remains sufficiently small. Alternatively, the end time T could be considered as a free parameter. Then, a further equation has to be added, e.g., $\|y(T) - \hat{y}\| = \varepsilon$, with ε fixed. For a time transformation $[0, \infty) \to [0, 1]$ see, e.g., Kunkel and von dem Hagen (25), Kitzhofer et al. (23).

3.2 Initializing the boundary value problem

In general a boundary value solver needs as an input argument an initial (approximative) function $y^{(0)}(\cdot)$. Depending on the problem this initial function can be a rather rough approximation, or has to be very close to the sought for solution. Anyhow, continuation techniques allow us to continue a solution once we have found at least one solution. Thus, we search for a solution we can easily get. The simplest possible solution of the BVP (26) is the equilibrium itself, provided we change the initial condition (26b) into

$$y^1(0) = \hat{y}^1. \tag{27}$$

For this BVP the constant path $y(\cdot) \equiv \hat{y}$ determines a solution and continuing this constant solution by changing the initial state we may finally find the solution we actually want to compute. The theoretical basis for this strategy can be found, e.g., in Winkler (33) or Krauskopf et al. (24).

3.3 Continuing the solution

In the simplest case we use a continuation technique with a fixed step width

$$\Delta := \frac{y_0^1 - \hat{y}^1}{n},\ n \in \mathbb{N}$$

and continue the solution of (26), with changing the initial conditions

$$y^1(0) = \zeta_k := \hat{y}^1 + k\Delta,\ k = 0, \ldots, n.$$

In fact the step width (Δ) can be made dependent on information about the solution process (for different specifications see App. C.1).

Subsequently, a solution path of the continuation process at step k is characterized by a superscript in round brackets $y^{(k)}(\cdot)$.

In the following sections we apply this method to problems derived from the optimal control problem (1), where the necessary optimality conditions provide the boundary conditions. This allows us to analyze paths switching between binding and not binding control constraints, or different paths starting at the same initial state and converging to different equilibria, and so forth.

4 Structural stable optimal vector field

In this section the main classes of numerical problems, where the optimal solution converges to an equilibrium, are presented. The analyzed optimal vector fields are structurally stable which means that, for an appropriate change of the parameter values, the optimal vector field does not undergo a local/global bifurcation. To give the reader a better intuition for the presented algorithms each case is accompanied by a specific example of the fishery model (9). For the base case the parameter values are taken from Tab. 1. Subsequently only the parameter values a and p are changed. Note that the parameter values were chosen to stress the numerical features and not with respect to a realistic scenario.

r	τ	c	a	p
0.1	0.25	0.375	7.5	0.1

Table 1: The parameter values for the base case, with a unique long run optimal equilibrium.

A thorough bifurcation analysis of the canonical system provides an indication on what we can expect for the optimal vector field. In App. A.4 this analysis can be found for the $p-a$ parameter space. These results suggest three different scenarios which are subsequently presented.

4.1 Case of a unique equilibrium

We subdivide this section into two parts. In the first part the calculations are done in detail for the fishery model and for specific parameter values. In the second part the problem is formulated for general problems.

Fishery model

In App. A.3 it is proved that for a unique equilibrium of the canonical system the corresponding stable path yields the optimal solution. For the parameter values of Tab. 1 we find the unique positive equilibrium

$$(\hat{x}, \hat{\lambda}) = (3.6803, 0.0432)$$

with the corresponding Jacobian matrix

$$J = \begin{pmatrix} -0.2460 & 6.7721 \\ 0.0081 & 0.3460 \end{pmatrix}.$$

The Jacobian J exhibits a positive and negative eigenvalue $\xi_1 = 0.4278$ and $\xi_2 = -0.3278$ proving the equilibrium to be a saddle point.

To calculate the stable path with, e.g. $x(0) = 10$, we solve the BVP (26) by applying a continuation algorithm presented (see App. C.1). Therefore, we fix the time horizon $T = 500$, and determine the vector (in general it is a matrix) F, which consists of the vector(s) orthogonal to the stable eigenspace. Since the eigenvector, corresponding to the negative eigenvalue, is given by

$$\nu = \begin{pmatrix} -0.9999 \\ 0.0121 \end{pmatrix} \quad \text{we find} \quad F = \begin{pmatrix} 0.0121 \\ 0.9999 \end{pmatrix}.$$

Thus, the BVP for the stable path becomes

$$\dot{x} = 500 \left(x \left(1 - \frac{x}{7.5} \right) - \frac{1}{0.625} \frac{x^2}{1+x^2} - \frac{x^2}{2}(0.1 - \lambda) \right) \tag{28a}$$

$$\dot{\lambda} = 500 \left(\lambda \left(-0.9 + \frac{2x}{7.5} + \frac{2x}{0.625(1+x^2)^2} \right) - \frac{x}{2}(0.1 - \lambda)^2 \right) \tag{28b}$$

$$x(0) = 10. \tag{28c}$$

$$(0.0121 \; 0.9999) \begin{pmatrix} x(1) - 3.6803 \\ \lambda(1) - 0.0432 \end{pmatrix} = 0 \tag{28d}$$

For the actual calculations we apply a fixed step width continuation strategy, with step width $\Delta = 0.01$. Thus we iteratively solve the BVP (28), where the initial state value (28c) is successively increased from the value at the equilibrium to 10, i.e., at step k the initial value is set to

$$x^{(k)}(0) = \hat{x}(1 - k\Delta) + x(0)k\Delta = 3.6803 + k0.0632, \; k = 0, 1, \ldots, 100.$$

The initial solution at step $k = 0$ is given by the constant path $x(t) = \hat{x}, \; t \in [0, 1]$. The result of this continuation is depicted in Fig. 1 for the steps $k = 1, 33, 66, 100$.

For the ODEs (28a) and (28b) we assumed that the control values lie in the interior of the control region, i.e., $u > 0$. This assumption may be violated during continuation and we have to check the admissibility of the calculated path. The next section addresses this problem by reformulating and extending the BVP (28).

Arcs of binding-not binding constraints To give an example of arcs, with binding and not binding (control) constraints, we calculate the saddle path starting at $x(0) = 0.1$. As in the previous case we start the continuation of the BVP (28) with the constant equilibrium solution. At each continuation step k the validity of the control constraint for the corresponding solution $(x^{(k)}(t), \lambda^{(k)}(t)),\ t \in [0,1]$ is checked, i.e, if

$$u^{\bullet(k)}(t) = \frac{x^{(k)}(t)}{2}(0.1 - \lambda^{(k)}(t)) \geq 0, \quad t \in [0,1] \tag{29}$$

holds. At step 38 of the continuation the control function (29) becomes negative, see Fig. 2b.

To proceed with the continuation, taking an arc of binding and not binding control constraint into account, the BVP (28) has to be extended. We assume that at time τ the optimal path switches from an arc of active to an arc of inactive control constraint, i.e., $u^*(t) = 0,\ t \leq \tau$ and $u^*(t) \geq 0,\ t \geq \tau$. Then we define

$$(x(t), \lambda(t)) := \begin{cases} (x_1(t), \lambda_1(t)) & t \leq \tau \\ (x_2(t), \lambda_2(t)) & t \geq \tau, \end{cases}$$

where $(x_1(t), \lambda_1(t))$ satisfies the ODEs (19) for $u^\bullet(t) = 0$ and $(x_2(t), \lambda_2(t))$ for $u^\bullet(t) = \frac{x(t)}{2}(p - \lambda(t))$. This yields a multi-point BVP which is transformed into a two-point BVP on $[0,1]$ (see App. B.1). For the transformed problem the switching time τ appears as an unknown parameter, yielding

$$\dot{x}_1 = \tau \left(x_1 \left(1 - \frac{x_1}{7.5}\right) - \frac{1}{0.625} \frac{x_1^2}{1 + x_1^2} \right) \tag{30a}$$

$$\dot{\lambda}_1 = \tau \left(\lambda_1 \left(-0.9 + \frac{2x_1}{7.5} + \frac{2x_1}{0.625(1 + x_1^2)^2} \right) \right) \tag{30b}$$

$$\dot{x}_2 = (500 - \tau) \left(x_2 \left(1 - \frac{x_2}{7.5}\right) - \frac{1}{0.625} \frac{x_2^2}{1 + x_2^2} - \frac{x_2^2}{2}(0.1 - \lambda_2) \right) \tag{30c}$$

$$\dot{\lambda}_2 = (500 - \tau) \left(\lambda_2 \left(-0.9 + \frac{2x_2}{7.5} + \frac{2x_2}{0.625(1 + x_2^2)^2} \right) - \frac{x_2}{2}(0.1 - \lambda_2)^2 \right) \tag{30d}$$

$$(0.0121\ 0.9999) \begin{pmatrix} x_2(1) - 3.6803 \\ \lambda_2(1) - 0.0432 \end{pmatrix} = 0 \tag{30e}$$

$$x_1(1) = x_2(0),\ \lambda_1(1) = \lambda_2(0) \tag{30f}$$

$$\frac{x_2(0)}{2}(p - \lambda_2(0)) = 0 \tag{30g}$$

$$x_1(0) = 0.1. \tag{30h}$$

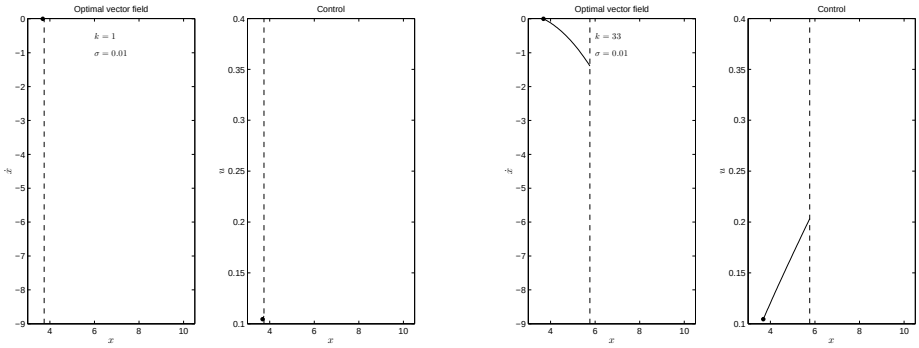

(a) Initialization

(b) Step 33

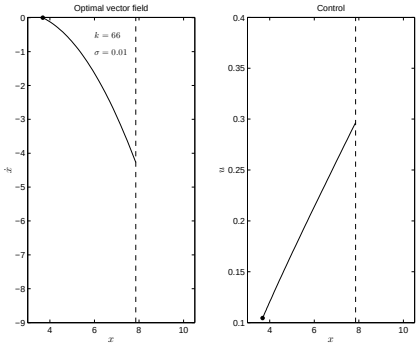

(c) Step 66

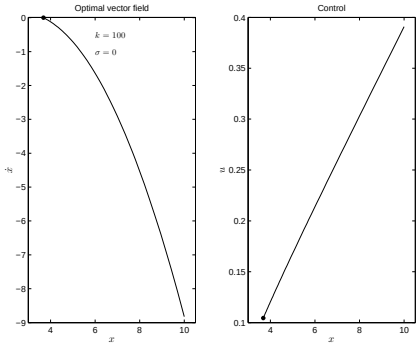

(d) Last step

Figure 1: The result of the continuation process is depicted at different steps. The left side of each subfigure shows the optimal vector field, and the right side shows the path in the state-control space. For the actual computation the parameter values are set to $a = 7.5$ and $p = 0.1$, the end time is fixed at $T = 500$ and $x(0) = 10$. (a) the equilibrium solution is used for initialization, (b)-(c) to continue the saddle path, (d) until the solution with $y_0^1 = 10$ is reached.

In total we have five unknown variables $(x_1, \lambda_1, x_2, \lambda_2, \tau)$, thus to state the BVP properly we have to provide five conditions. Since the second arc converges to the equilibrium (30e) states the usual asymptotic transversality condition. State and costate are continues at the switching time which, due to the time transformation, yields (30f). The last equation (30h) provides the initial condition. Finally, (30g) guarantees the continuity of the optimal control at the switching time τ, and provides the condition for the unknown switching time τ.

To start the continuation for BVP (30) we use the solution of the last step k_0, where the control constraint was violated. For reasons of simplicity we assume that for the time discretization $t_i,\ i = 0, \dots, n$ the violation appears at the initial time, i.e., $u^{(k_0)}(0) < 0$ and $u^{(k_0)}(t_i) > 0,\ i > 0$. Then, we define an initial function for (30) by setting

$$\tau := 0 \tag{31a}$$

$$(x_1^{(0)}(t), \lambda_1^{(0)}(t)) := (x^{(k_0)}(0), \lambda^{(k_0)}(0)),\ t \in [0, 1] \tag{31b}$$

$$(x_2^{(0)}(t), \lambda_2^{(0)}(t)) := (x^{(k_0)}(t), \lambda^{(k_0)}(t)),\ t \in [0, 1]. \tag{31c}$$

and the initial condition

$$x_1^{(0)}(0) = x^{(k_0)}(0). \tag{31d}$$

Using these functions the continuation process can be proceeded solving the extended BVP (30).

The first arc of the solution path now has to satisfy the non-negativity of the corresponding Lagrangian multiplier and the second arc has to satisfy the control constraint. Therefore, both conditions have to be checked during continuation. For the actual computation the Lagrangian multiplier becomes negative at step $k = 72$, see Fig. 2c.

To calculate the path consisting of three arcs, where the first arc has positive control, the second arc zero control and the third arc positive control again we have to consider switching times τ_1 and τ_2. Analogous to the previous case the problem can be formulated as

$$(x(t), \lambda(t)) := \begin{cases} (x_1(t), \lambda_1(t)) & t \leq \tau_1 \\ (x_2(t), \lambda_2(t)) & \tau_1 \leq t \leq \tau_2 \\ (x_3(t), \lambda_3(t)) & t \geq \tau_2, \end{cases}$$

and extend, after time normalization, the BVP (30) to

$$\dot{x}_1 = \tau_1 \left(x_1 \left(1 - \frac{x_1}{7.5} \right) - \frac{1}{0.625} \frac{x_1^2}{1 + x_1^2} - \frac{x_1^2}{2} (0.1 - \lambda_1) \right) \tag{32a}$$

$$\dot{\lambda}_1 = \tau_1 \lambda_1 \left(-0.9 + \frac{2x_1}{7.5} + \frac{2x_1}{0.625(1 + x_1^2)^2} - \frac{x_1}{2} (0.1 - \lambda_1)^2 \right) \tag{32b}$$

$$\dot{x}_2 = (\tau_2 - \tau_1) \left(x_2 \left(1 - \frac{x_2}{7.5} \right) - \frac{1}{0.625} \frac{x_2^2}{1 + x_2^2} \right) \tag{32c}$$

$$\dot{\lambda}_2 = (\tau_2 - \tau_1) \lambda_2 \left(-0.9 + \frac{2x_2}{7.5} + \frac{2x_2}{0.625(1 + x_2^2)^2} \right) \tag{32d}$$

$$\dot{x}_3 = (500 - \tau_2) \left(x_3 \left(1 - \frac{x_3}{7.5} \right) - \frac{1}{0.625} \frac{x_3^2}{1 + x_3^2} - \frac{x_3^2}{2} (0.1 - \lambda_3) \right) \tag{32e}$$

$$\dot{\lambda}_3 = (500 - \tau_2) \lambda_3 \left(-0.9 + \frac{2x_3}{7.5} + \frac{2x_3}{0.625(1 + x_3^2)^2} - \frac{x_3}{2} (0.1 - \lambda_3)^2 \right) \tag{32f}$$

$$(0.0121 \ 0.9999) \begin{pmatrix} x_3(1) - 3.6803 \\ \lambda_3(1) - 0.0432 \end{pmatrix} = 0 \tag{32g}$$

$$x_1(1) = x_2(0), \ \lambda_1(1) = \lambda_2(0), \ x_2(1) = x_3(0), \ \lambda_2(1) = \lambda_3(0) \tag{32h}$$

$$\frac{x_3(0)}{2} (p - \lambda_3(0)) = 0 \tag{32i}$$

$$- x_2(0)(p - \lambda_2(0)) = 0 \tag{32j}$$

$$x_1(0) = 0.1. \tag{32k}$$

The explanation of 32a–32i and initial condition (32k) is straight forward from the previous example. Equation (32j) expresses the continuity of the Lagrangian multiplier (18) at the switching time τ_1.

To start the continuation of BVP (32) an initial function can be constructed analogous to (31). Using (32) the solution starting at $x_1(0) = 0.1$ can be computed and the final result is depicted in Fig. 2d.

General model

For the general problem (1) we have to distinguish between two cases, namely the case of the control value lying in the interior of the control constraint, i.e., $k(x, u) > 0$, and the case of the control value lying at the boundary of the control constraint, i.e., $k(x, u) = 0$. For notational simplicity we assume that only one constraint exists, i.e., $k(x, u) \in \mathbb{R}$.

To differentiate between the two cases we write for the canonical system corresponding to the interior case

$$\dot{y}(t) = g(y(t)), \tag{33}$$

where $y := (x, \lambda) \in \mathbb{R}^{2n}$.

For the boundary case we set $z := (x, \lambda) \in \mathbb{R}^{2n}$ and write for the canonical system

$$\dot{z}(t) = h(z(t)), \tag{34}$$

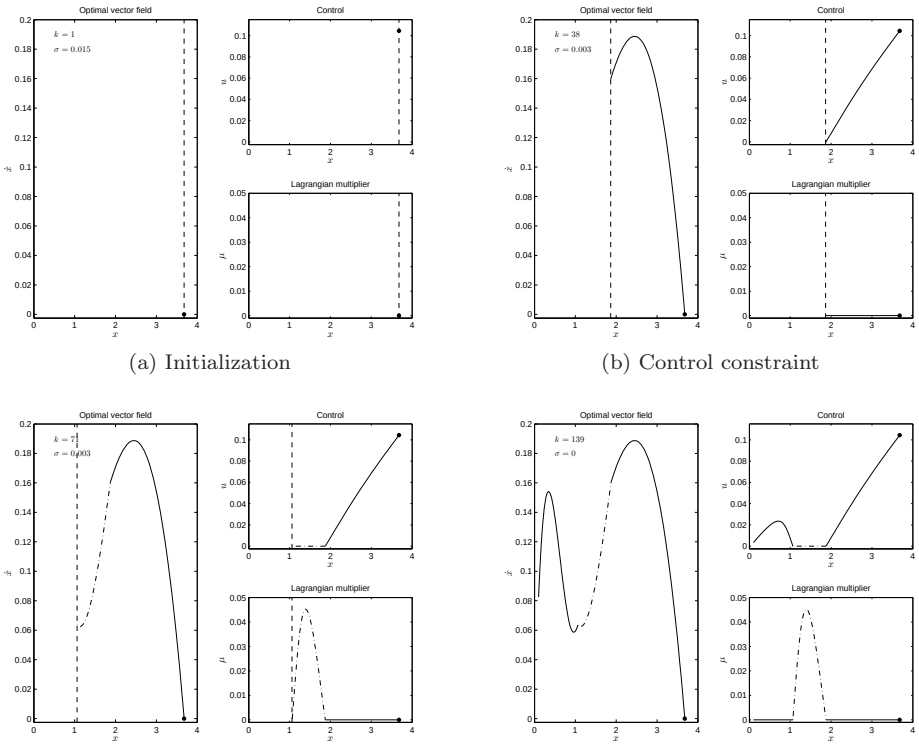

(a) Initialization (b) Control constraint

(c) Positive multiplier (d) Final path

Figure 2: The continuation process for arcs with binding and not binding control constraints is depicted. The left side of each subfigure shows the optimal vector field, and the right side shows the control and the Lagrangian multipliers, respectively. For the actual computation the parameter values are set to $a = 7.5$ and $p = 0.1$, the end time is fixed at $T = 500$ and $x(0) = 0.1$. (a) Starting at the equilibrium solution a continuation process using BVP (28) is started. (b) During this process first a violation of the control constraint is detected and therefore the BVP (30) is used, (c) thereafter the Lagrangian multiplier becomes negative and three arcs have to be considered by solving BVP (32). (d) shows the sought for solution path. The dashed-dotted arc denotes the part of the optimal solution, where the optimal control is at its boundary, i.e. $u^* = 0$.

where additionally $z(t)$ satisfies the control constraint sharply, i.e, $k(z(t)) = 0$.

Let us assume that the interior system (33) exhibits a (unique) saddle point $\hat{y}$ and has n negative eigenvalues. Next we want to find the stable path starting at some initial value $y^1(0) = \zeta \in \mathbb{R}^n$. To validate that the solution path $y(\cdot)$ satisfies the constraint (1d) we define a tolerance $\varepsilon > 0$ and check that

$$k(y(t)) \geq \varepsilon, \quad \text{holds for all} \quad t. \tag{35}$$

Using the algorithm presented in Sect. 3, the following BVP has to be solved by continuation

$$\dot{y}(t) = Tg(y(t)),\ t \in [0,1] \tag{36a}$$
$$y^1(0) = \zeta \tag{36b}$$
$$F'(y(1) - \hat{y}) = 0 \quad \text{with} \quad F \in \mathbb{R}^{2n \times n}. \tag{36c}$$

During the continuation process (35) is checked. Let the constraint (35) be violated at some step N, where for reasons of simplicity we assume that the violation occurs at a time interval $[0, t_v]$, i.e., $k(y(t)) < \varepsilon,\ t \in [0, t_v)$ and $k(y(t)) \geq \varepsilon,\ t \in [t_v, T]$.

To handle this case we split the solution path into two arcs. The first arc with the control value at the boundary and the second arc with the control value lying in the interior of the control region. Thus, we can set up an extended BVP with additional boundary conditions at the switching point. Reformulating the multi-point problem as a two-point problem (see App. B.1) and denoting the unknown switching time as τ the BVP becomes

$$\dot{z}(t) = \tau h(z(t)),\ t \in [0,1] \tag{37a}$$
$$\dot{y}(t) = (T - \tau) g(y(t)),\ t \in [0,1] \tag{37b}$$
$$z(1) = y(0) \tag{37c}$$
$$k(y(0)) = 0 \tag{37d}$$
$$z^1(0) = \zeta \tag{37e}$$
$$F'(y(1) - \hat{y}) = 0. \tag{37f}$$

The new condition (37c) reflects the continuity of the state and costate at the switching point and (37d) the continuity of the control.

Remark 4 (Continuity of the control). The boundary condition (37d) only holds true if the continuity of the control function is guaranteed. This is, e.g. assured by the uniqueness of the optimal control value. In cases of a possibly discontinuous control (37d) has to be replaced by the continuity of the Hamiltonian at the switching point, i.e.

$$\mathcal{H}(y(0)) = \mathcal{H}(z(1)). \tag{38}$$

Remark 5 (Switching from the boundary to the interior control region). For an arc with the control value lying at the boundary of the control region the Lagrangian multiplier $\psi(\cdot)$ has to be non-negative. Therefore this condition has

to be checked during continuation. In case that this condition is violated the same procedure yields an extended BVP, where condition (37d) is then replaced by the condition

$$\psi(z(1)) = 0. \tag{39}$$

In cases, where the continuity of the Lagrangian multiplier cannot be guaranteed (39) has to be replaced by (38).

4.1.1 Initialization of (37)

To start the continuation for the system (37) a function $(z(t), y(t))'$, $t \in [0,1]$ has to be provided. Using the last computed solution path $y^{(N)}(\cdot)$ and normalizing the time intervals $[0, t_v]$, and t_v, T to the unit interval, yields

$$\begin{pmatrix} z(t) \\ y(t) \end{pmatrix} = \begin{pmatrix} y^{(N)}(tt_v) \\ y^{(N)}(t_v + t(T - t_v)) \end{pmatrix} \quad t \in [0,1] \quad \text{and} \quad \tau = t_v.$$

For the numerical computations of $(z(t), y(t))$ starting at a time grid $0 = t_0 < t_1 < \ldots < t_m = 1$ the time transformation requires that the solution $y^{(N)}(\cdot)$ is evaluated at the time points $t_i t_v$ and $t_v + t_i(T - t_v)$, $i = 0, \ldots, k$.

We note that the first arc $z(t)$ does, in general, not satisfy (37a). But if t_v is small enough this function can serve as a good approximation for the solution of the BVP (37) (see Fig. 2).

4.2 Multiple equilibria

In some optimal control problems of type (1) the canonical system exhibits multiple equilibria. Therefore, another basic issue is the identification of the optimal solution among different extremals. In case that multiple optimal solutions exist, the main problem is to locate the so called indifference threshold point(s). These are points in the state space at which different paths yield the same objective value, i.e., each of these paths is equally optimal. For a detailed discussion of such points see Kiseleva and Wagener (22), Kiseleva (21) and Grass et al. (16).

4.2.1 One superior solution

For a concrete example in the fishery model (9) we choose $p = 0.25$ in the fishery model (see Fig. 15). For this parameter value we find three (strictly positive) equilibria for the canonical system

$$\begin{pmatrix} \hat{x}_1 \\ \hat{\lambda}_1 \end{pmatrix} = \begin{pmatrix} 0.9101 \\ 0.069381 \end{pmatrix}, \quad \begin{pmatrix} \hat{x}_2 \\ \hat{\lambda}_2 \end{pmatrix} = \begin{pmatrix} 1.2884 \\ 0.16737 \end{pmatrix}, \quad \begin{pmatrix} \hat{x}_3 \\ \hat{\lambda}_3 \end{pmatrix} = \begin{pmatrix} 3.2616 \\ 0.17843 \end{pmatrix}.$$

with corresponding eigenvalues

$$\xi_1 = \begin{pmatrix} -0.2439 \\ 0.3439 \end{pmatrix}, \quad \xi_2 = \begin{pmatrix} 0.0500 + 0.2301\mathrm{i} \\ 0.0500 - 0.2301\mathrm{i} \end{pmatrix}, \quad \xi_3 = \begin{pmatrix} -0.4326 \\ 0.5326 \end{pmatrix}.$$

Thus, only $(\hat{x}_1, \hat{\lambda}_1)$ and $(\hat{x}_3, \hat{\lambda}_3)$ are saddle points, $(\hat{x}_2, \hat{\lambda}_2)$ is an unstable focus and can therefore be discarded as a long run optimal solution. To determine if one of the stable paths is superior to the other we have to compare the corresponding objective values. Therefore, we use the continuation algorithm and BVP presented in the previous section to determine the paths with initial value $x(0) = \hat{x}_1$ and converging to $(\hat{x}_3, \hat{\lambda}_3)$ and vice versa for $x(0) = \hat{x}_3$ converging to $(\hat{x}_1, \hat{\lambda}_1)$.

For demonstration purposes we explicitly write down the BVP for the first continuation and use an adaptive step width strategy (see App. C.1), which allows us to follow a backbending of the stable path.[4] Thus the continuation parameter γ is now free and one more condition is specified (40e). Given that we already solved the problem for continuation step $k-1$ and $k \geq 1$ the BVP for step $k+1$ becomes[5]

$$\dot{x} = 500 \left(x \left(1 - \frac{x}{7.5} \right) - \frac{1}{0.625} \frac{x^2}{1+x^2} - \frac{x^2}{2}(0.25 - \lambda) \right) \tag{40a}$$

$$\dot{\lambda} = 500 \left(\lambda \left(-0.9 + \frac{2x}{7.5} + \frac{2x}{0.625(1+x^2)^2} \right) - \frac{x}{2}(0.25 - \lambda)^2 \right) \tag{40b}$$

$$(-0.0829 \; 0.9966) \begin{pmatrix} x(1) - 0.9101 \\ \lambda(1) - 0.069381 \end{pmatrix} = 0 \tag{40c}$$

$$x(0) = \hat{x}_1(1-\gamma) + \gamma \hat{x}_1 = 0.9101 + 2.3515\gamma \tag{40d}$$

$$V' \begin{pmatrix} x(0) - x^{(k)}(0) \\ \lambda(0) - \lambda^{(k)}(0) \end{pmatrix} - \sigma = 0 \tag{40e}$$

with

$$V := \begin{pmatrix} x^{(k)}(0) - x^{(k-1)}(0) \\ \lambda^{(k)}(0) - \lambda^{(k-1)}(0) \end{pmatrix} / \left\| \begin{pmatrix} x^{(k)}(0) - x^{(k-1)}(0) \\ \lambda^{(k)}(0) - \lambda^{(k-1)}(0) \end{pmatrix} \right\|.$$

For the geometric interpretation of (40e) see Fig. 3a. The searching direction for the initial point of the stable path depends on the previously detected solutions and therefore allows to follow the stable path even if it is backbending, cf. Fig. 3b.

The computation of the stable path corresponding to $(\hat{x}_3, \hat{\lambda}_3)$ is done in an analogous way. In Fig. 4 the result of these computations are shown, together with the corresponding objective values. Comparing the objective values we find that the stable path $(\hat{x}_3, \hat{\lambda}_3)$ is superior and therefore yields the unique optimal solution. Consequently, the optimal vector field exhibits the globally stable equilibrium $\hat{x}_3$.

4.2.2 Indifference thresholds

Next we analyze the case where none of the stable paths can be continued to the other equilibrium state but parts of the stable paths overlap in the projection

[4] For autonomous one-dimensional models backbending paths are in general not optimal, Hartl (see e.g. 18)

[5] For the first two continuation steps a fixed step width algorithm can be used.

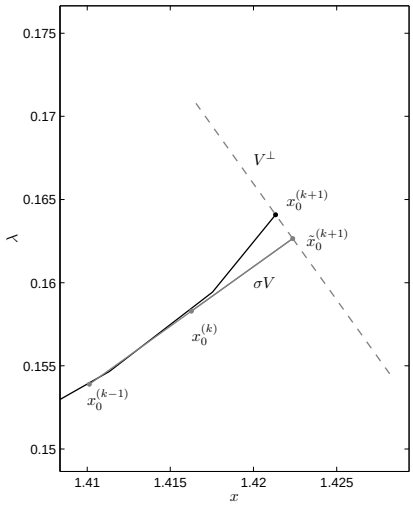

(a) Adaptive Step

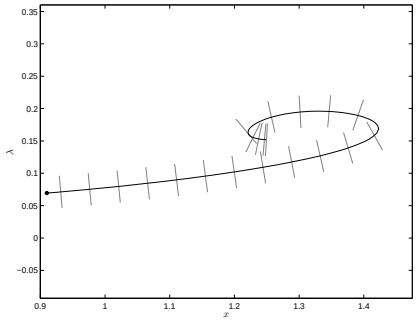

(b) Backbending

Figure 3: For the adaptive continuation step in (a) the initial point for step $k+1$ is predicted from the secant of the two previous initial points. The exact initial point is then searched along the orthogonal direction to the secant. The adaptive continuation process allows the continuation of a backbending solution path, which is depicted in (b).

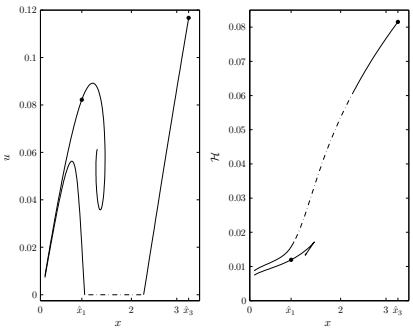

(a) Stable paths

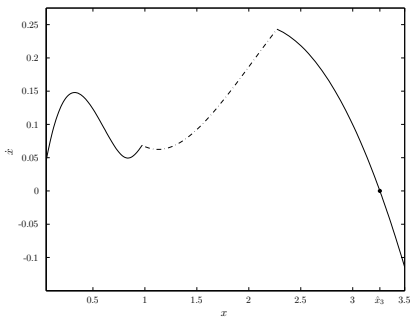

(b) Continuous vector field

Figure 4: (a) depicts the stable paths of the two saddles (located at $\hat{x}_1$ and $\hat{x}_3$) (left side) together with the corresponding objective values (right side). Since the saddle path converging to the equilibrium at $\hat{x}_3$ is superior the (b) optimal vector field consists of the unique stable equilibrium $\hat{x}_3$. For the actual numerical calculations the parameter base case value are used and $p = 0.25$.

to the state space. For that we present a concrete example in our fishery model and summarize the results then for the general case.

Fishery model

We increase the parameter value p to one, where the bifurcation diagram of the canonical system (Fig. 15 in App. A.4) shows that also three strictly positive equilibria exist. We find that

$$\begin{pmatrix}\hat{x}_1\\ \hat{\lambda}_1\end{pmatrix} = \begin{pmatrix}0.63252\\ 0.39029\end{pmatrix}, \quad \begin{pmatrix}\hat{x}_3\\ \hat{\lambda}_3\end{pmatrix} = \begin{pmatrix}3.0753\\ 0.92232\end{pmatrix}$$

are saddles and the third is an unstable focus. Following the steps of the previous section we find that for this case none of the stable paths yields a globally superior solution and the Hamiltonian evaluated along the stable paths (cf. Fig. 5) intersect at some point. Since the Hamiltonian value (divided by the discount rate) yields the objective value this means that starting at the state value of this intersection point, both solutions are equally optimal.

Next we describe the steps to compute the exact position of this so-called indifference threshold.

Step 1 First, we calculate the stable paths for the two saddle points, this is not explicitly carried out, but yield the two stable manifolds $(x_1, \lambda_1(x_1))$ and $(x_2, \lambda_2(x_2))$, as curves in the state-costate space. In Fig. 5a we see that there exists an interval I in the state space, where for $x \in I$ both stable manifolds exist. The approximate intersection point $\tilde{x}$ of the functions $\mathcal{H}(x, \lambda_1(x))$ and $\mathcal{H}(x, \lambda_2(x)),\ x \in I$, can be determined by some numerical procedure.

Step 2 Next, we calculate the stable paths starting at the initial state $\tilde{x}$ (cf. Fig. 5b). This is straight forward and we can use this solution as the initial functions for the next step. In the actual case the calculations reveal that the stable path of the third equilibrium consists of two arcs, with binding and not binding control constraint, which we subsequently denote as $(x_i(\cdot), \lambda_i(\cdot)),\ i = 1, 2$. The control along the stable path of the first equilibrium is strictly positive and the path will subsequently be denoted as $(x_3(\cdot), \lambda_3(\cdot))$. In both cases the time horizon was truncated at $T = 500$.

Step 3 To formulate the BVP for the exact location of the indifference threshold we assemble the results described so far. It consists of the ODEs

$$\dot{x}_1 = \tau \left(x_1 \left(1 - \frac{x_1}{7.5} \right) - \frac{1}{0.625} \frac{x_1^2}{1 + x_1^2} \right) \tag{41a}$$

$$\dot{\lambda}_1 = \tau \lambda_1 \left(-0.9 + \frac{2x_1}{7.5} + \frac{2x_1}{0.625(1 + x_1^2)^2} \right) \tag{41b}$$

$$\dot{x}_2 = (500 - \tau) \left(x_2 \left(1 - \frac{x_2}{7.5} \right) - \frac{1}{0.625} \frac{x_2^2}{1 + x_2^2} - \frac{x_2^2}{2}(1 - \lambda_2) \right) \tag{41c}$$

$$\dot{\lambda}_2 = (500 - \tau) \lambda_2 \left(-0.9 + \frac{2x_2}{7.5} + \frac{2x_2}{0.625(1 + x_2^2)^2} - \frac{x_2}{2}(1 - \lambda_2)^2 \right) \tag{41d}$$

$$\dot{x}_3 = 500 \left(x_3 \left(1 - \frac{x_3}{7.5} \right) - \frac{1}{0.625} \frac{x_3^2}{1 + x_3^2} - \frac{x_3^2}{2}(1 - \lambda_3) \right) \tag{41e}$$

$$\dot{\lambda}_3 = 500 \lambda_3 \left(-0.9 + \frac{2x_3}{7.5} + \frac{2x_3}{0.625(1 + x_3^2)^2} - \frac{x_3}{2}(1 - \lambda_3)^2 \right) \tag{41f}$$

the asymptotic boundary conditions for the two stable paths

$$(0.1516 \ 0.9884) \begin{pmatrix} x_2(1) - 3.0753 \\ \lambda_2(1) - 0.9223 \end{pmatrix} = 0 \tag{41g}$$

$$(-0.1375 \ 0.9905) \begin{pmatrix} x_3(1) - 0.63252 \\ \lambda_3(1) - 0.39029 \end{pmatrix} = 0 \tag{41h}$$

and the switching conditions from the boundary to the interior arc

$$\frac{x_2(0)}{2}(1 - \lambda_2(0)) = 0 \tag{41i}$$

$$x_1(1) = x_2(0), \ \lambda_1(1) = \lambda_2(0). \tag{41j}$$

Finally we have to specify the conditions characterizing solutions starting at an indifference threshold. The seven unknowns, six variables of the ODEs and the switching time τ, are accompanied by five boundary conditions. Thus, two further conditions are missing, which are given by

$$x_1(0) = x_3(0) \tag{41k}$$

$$\mathcal{H}(x_1(0), u(x_1(0), \lambda_1(0)), \lambda_1(0)) = \mathcal{H}(x_3(0), u(x_3(0), \lambda_3(0)), \lambda_3(0)). \tag{41l}$$

The first condition (41k) states that the indifference threshold is the initial point for the two saddle paths and (41l) reflects the fact that both solutions yield the same objective value.

The final result of the computation is shown in Fig. 5c. This reveals that the optimal vector field consists of two locally stable equilibria and their basin of attraction is separated by the indifference threshold. At the indifference threshold the optimal vector field is discontinuous (cf. Fig. 5c).

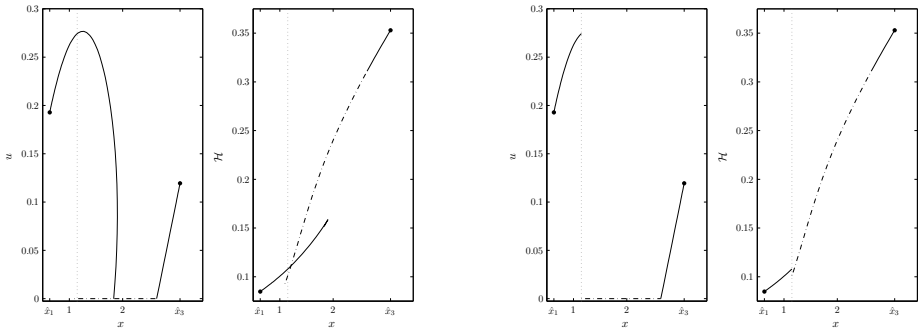

(a) Intersecting Hamiltonian

(b) Approximate solution

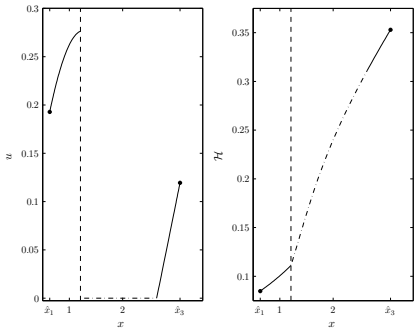

(c) Indifference threshold

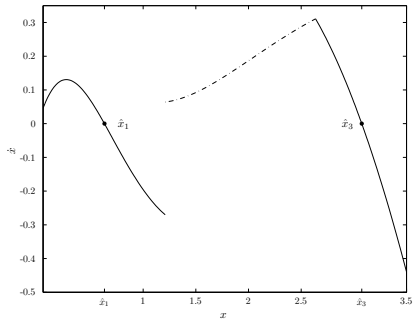

(d) Discontinuous vector field

Figure 5: The numerical detection of an indifference threshold is depicted. (a) shows the stable paths and intersection point of the Hamiltonian evaluated along the candidate solutions (see (8)). (b) the state value of the (numerically approximated) intersection point (dotted line). The stable paths starting at this intersection point are used as an approximate solution. (c) the exact location of the indifference threshold is found by solving the BVP (42) and is denoted by the dashed line. (d) the optimal vector field is discontinuous at the indifference threshold. For the actual numerical calculations $p = 1$.

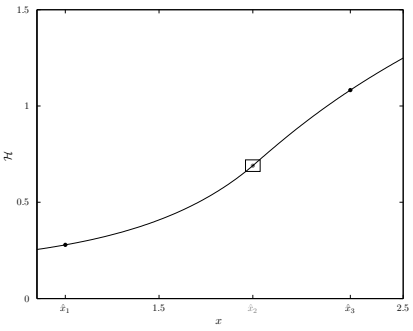

(a) Overlap near unstable node

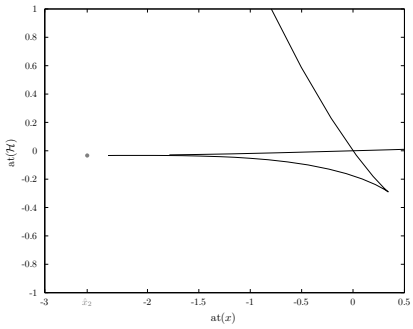

(b) Intersecting Hamiltonian

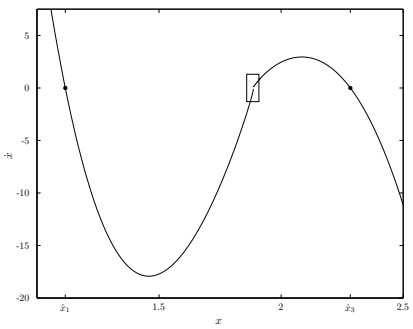

(c) Indifference threshold

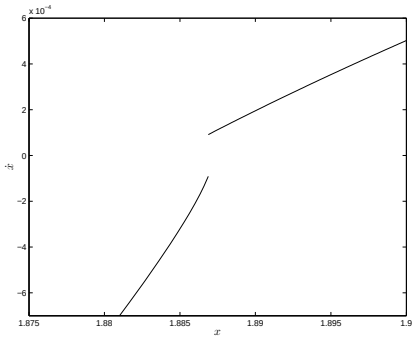

(d) Discontinuous optimal vector field

Figure 6: The case of an indifference threshold near an unstable node is depicted. The stable paths (a) have an overlap in the state space near the unstable node. In this overlap region (b) the Hamiltonians intersect, yielding an indifference threshold. The optimal vector field exhibits two stable equilibria (c) and is discontinuous (d) at the indifference threshold. For the actual calculations the parameter values were specified as $p = 0.03$ and $a = 5.895$.

Unstable node In the literature the existence of an indifference threshold is often seen as a result of an unstable focus lying between two saddle points. But indifference thresholds may also appear in case of an unstable node as depicted in Fig. 6. For the numerical calculation the parameter values of the base case were changed for $p = 0.03$ and $a = 5.895$. The concrete calculation is omitted since it is analogous to the last example.

General case

For the general model (1) we assume the existence of an indifference threshold x_I, where it is equally optimal to converge either to the equilibrium $\hat{y}_1$ or to $\hat{y}_2$. Then, two solutions $y_1(\cdot)$ and $y_2(\cdot)$ start at the indifference threshold and

exhibit the same objective value yielding

$$y_1^1 = y_2^1 = x_I \in \mathbb{R}^n \quad \text{and} \quad \mathcal{H}(y_1(0)) = \mathcal{H}(y_2(0)).$$

These properties allow us to formulate the BVP characterizing an indifference threshold. For fixed but maybe different truncation times T_1 and T_2 the solutions starting at an indifference threshold are characterized by the following BVP

$$\dot{y}_1(t) = T_1 f_1(y_1(t)),\ t \in [0,1] \tag{42a}$$
$$\dot{y}_2(t) = T_2 f_2(y_2(t)),\ t \in [0,1] \tag{42b}$$
$$y_1^1(0) = y_2^1(0) \tag{42c}$$
$$\mathcal{H}(y_1(0)) = \mathcal{H}(y_2(0)) \tag{42d}$$
$$F_1'(y_1(1) - \hat{y}_1) = 0 \tag{42e}$$
$$F_2'(y_2(1) - \hat{y}_2) = 0. \tag{42f}$$

The two ODEs (42a) and (42b) denote the two different solutions.[6] The conditions (42c) and (42d) are the decisive properties of the indifference threshold. Finally (42e) and (42f) are the usual asymptotic transversality conditions for the two solutions converging to the (different) equilibria $\hat{y}_1$ and $\hat{y}_2$.

To determine an initial solution for the BVP (42) we can use the results from the previous continuations, where we determined the intersection point of the Hamiltonian evaluated along the two paths. The solutions starting at this approximated intersection point are calculated and can then be used as an initial solution for (42).

Remark 6. In the one dimensional case it usually suffices to determine the indifference threshold as the intersection point of the Hamiltonian. Anyhow the formulation as a BVP admits an immediate way to continue the indifference threshold for varying parameters. For higher dimensional models this formulation is essential to determine the analogous indifference curve/surface via continuation.

4.2.3 Threshold point and time horizon

In Sect. 4.2.2 we mentioned the case, where, in the canonical system, an unstable node is adjacent to two saddles and gives rise to an indifference threshold in the optimal vector field. But in general an unstable node in the canonical system can become an unstable equilibrium of the optimal vector field. For a concrete numerical example in the fishery model we change the parameter values $p = 0.03$ and $a = 5.88$. In that case three equilibria

$$\begin{pmatrix} \hat{x}_1 \\ \hat{\lambda}_1 \end{pmatrix} = \begin{pmatrix} 1.1115 \\ 0.0022538 \end{pmatrix}, \quad \begin{pmatrix} \hat{x}_2 \\ \hat{\lambda}_2 \end{pmatrix} = \begin{pmatrix} 1.9585 \\ 0.010689 \end{pmatrix}, \quad \begin{pmatrix} \hat{x}_3 \\ \hat{\lambda}_3 \end{pmatrix} = \begin{pmatrix} 2.1929 \\ 0.0089891 \end{pmatrix}$$

[6] Note that the ODEs (42a) and (42b) can consist of different arcs exhibiting binding and not binding control constraints.

with corresponding eigenvalues

$$\xi_1 = \begin{pmatrix} -0.1182 \\ 0.2182 \end{pmatrix}, \quad \xi_2 = \begin{pmatrix} 0.0183 \\ 0.0817 \end{pmatrix}, \quad \xi_3 = \begin{pmatrix} -0.0176 \\ 0.1176 \end{pmatrix}.$$

exist. To check if the unstable node is an equilibrium solution we consider the second derivative of the maximized Hamiltonian with respect to x, i.e., $\mathcal{H}_{xx}(x, u(x, \lambda), \lambda)$, evaluated at the unstable node yields

$$\mathcal{H}_{xx}(1.9585, 0.0189, 0.010689) = -2.7085 \times 10^{-4} < 0$$

and is therefore strictly negative. Thus, the equilibrium solution satisfies the Arrow sufficiency conditions and is therefore the unique optimal solution with $x(0) = 1.9585$. For initial states $x(0)$ left of $\hat{x}_2$ the stable path converging to $(\hat{x}_1, \hat{\lambda}_1)$, right of $\hat{x}_2$ the stable path converging to $(\hat{x}_3, \hat{\lambda}_3)$ yields the optimal solution. Consequently, the optimal vector field is continuous as illustrated in Fig. 8, exhibiting two stable and one unstable equilibria, which justifies the denotation as threshold point for the unstable equilibrium $\hat{x}_2$.

For the calculation of the stable paths in the vicinity of the unstable node $\hat{x}_2$ we use the usual continuation process of the corresponding BVP and start with a truncation time $T = 100$. The initial states, from which the stable paths start, are taken as $\hat{x}(0) = (1 \mp \varepsilon)\hat{x}_2$ with $\varepsilon = 10^{-4}$.

In these cases the value of the truncation time becomes crucial since paths starting "near" the unstable node remain there for "long". Thus a too short truncation time may yield a solution which ends up at the linear stable manifold but not "near" the saddle point. This happens for the truncation time $T = 100$ and is illustrated in Fig. 7a,b.

To find the correct solution truncation time is increased from $T = 100$ to $T = 250$. Therefore continuation is used, where the initial state is fixed and the time horizon T is successively increased (cf. Fig. 7c,d.)

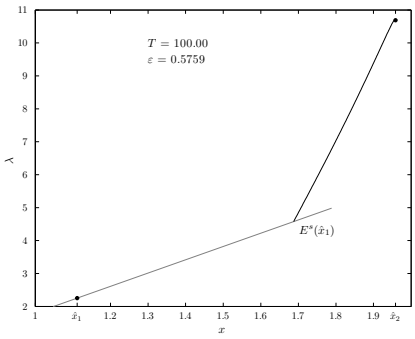

(a) Initial state near $\hat{x}_2$

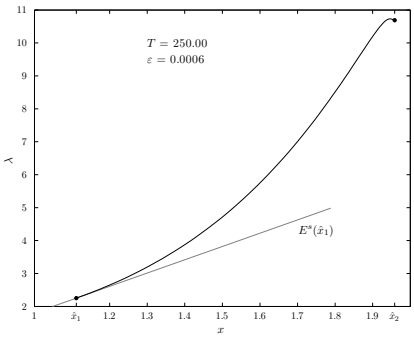

(b) Increased truncation time

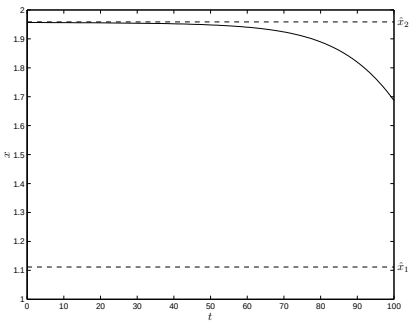

(c) Timepath near $\hat{x}_2$

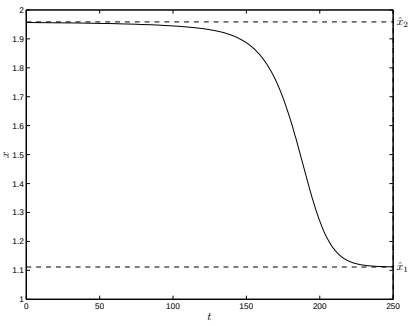

(d) Increased truncation time

Figure 7: The solution for time horizon $T = 100$ and $T = 250$ is depicted in the phase portrait (a,b) and in the time domain (c,d). The solution (a) ends at the stable eigenspace (black line) but ends not "near" the equilibrium. The reason can be seen in (c) since the path stays for "long" near the unstable equilibrium. In (b) and (d) the solution is depicted after the continuation process where the truncation time was increased up to $T = 250$. The time span is now long enough to satisfy numerically both effects, staying near the unstable equilibrium and ending near the saddle point.

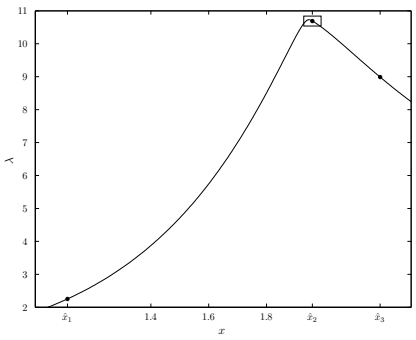

(a) Continuous costate

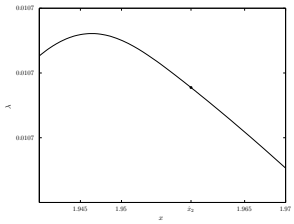

(b) Blow up

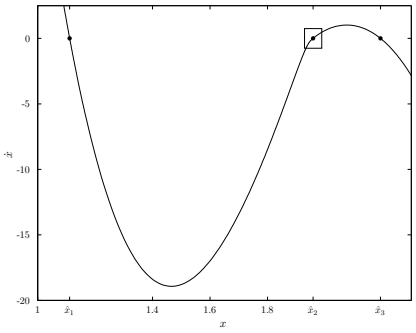

(c) Continuous optimal vector field

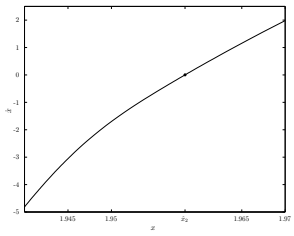

(d) Blow up

Figure 8: The case of a threshold point is depicted. The stable manifolds (a) are continuously connect at the unstable node as the blow up (b) shows. The optimal vector field (c) exhibits two stable and one unstable equilibrium and is continuous at the unstable equilibrium (d). For the actual calculations the parameter values were specified as $p = 0.03$ and $a = 5.88$.

5 Bifurcations of the optimal vector field

In the previous sections we presented the numerical algorithms for cases where the optimal vector field was structurally stable under "small" perturbations of the parameter values. Next, we have a closer look to the switching between two qualitatively different optimal vector fields in the parameter space. Thus, we calculate the bifurcations of the optimal vector field. In Kiseleva and Wagener (22) and Kiseleva (21) the authors give a fairly general classification of possible codimension one and two bifurcations of an optimal vector field for a one state optimal control problem. Using these results we show how to set up the boundary conditions, which characterize the different types of bifurcations. Once more we apply these numerical algorithms to the fishery model and can finally put together the bifurcation diagram of the optimal system (see Fig. 14).

5.1 Indifference attractor bifurcation (IAB)

In Wagener (31) it has been proved that a heteroclinic bifurcation, where a stable and unstable path of two saddles coincide (see Fig. 10), can give rise to the emergence of indifference thresholds. In Kiseleva and Wagener (22) and Kiseleva (21) the IAB was classified as one of the possible codimension one bifurcations, which an optimal vector field can undergo.

Fishery model

In Fig. 9 a typical situation in the vicinity of an indifference threshold is depicted ($a \in [9, 7.5]$). We remind the reader that within this interval of parameter a the number and stability properties of the equilibria of the canonical system do not change, i.e., there exist two saddles and one unstable focus. Thus, the local behavior of the extremal paths remain the same, but the global geometry of the (un)stable paths changes.

For higher values of a the stable path of the saddle at the right covers the entire state space and lies above the unstable path of the left equilibrium (cf. Fig. 9a,d). For lower values of a the stable and unstable path interchanged their relative position (cf. Fig. 9c,f). At a specific value for a the stable and unstable path coincide and constitute a heteroclinic connection, (cf. Fig. 9b,e). We will next show how the exact value of a, where the heteroclinic connection appears, can be determined.

A heteroclinic connection, denoted by $\Gamma \subset \mathbb{R}^2$, between the equilibria $(\hat{x}_1, \hat{\lambda}_1)$ and $(\hat{x}_2, \hat{\lambda}_2)$ is characterized by the proeprty that starting at any point $(x(0), \lambda(0)) \in \Gamma$ the solution converges to one of the equilibria in positive time and to the other equilibrium in negative time, i.e.

$$\lim_{t\to\infty}(x(t), \lambda(t)) = (\hat{x}_1, \hat{\lambda}_1), \quad \lim_{t\to-\infty}(x(t), \lambda(t)) = (\hat{x}_2, \hat{\lambda}_2).$$

The freedom in choosing any point on Γ yields an indeterminacy. To get rid of this indeterminacy one further equation has to be provided. For the actual

computation we therefore fix the state value at $x_0 = 2$. Next we choose $a = 7.5$ and calculate the (un)stable path for the equilibria

$$(\hat{x}_1, \hat{\lambda}_1) = (0.63252, 0.39029) \quad \text{and} \quad (\hat{x}_2, \hat{\lambda}_2) = (3.0753, 0.92232),$$

starting at $\hat{x}(0) = 2$. The result of the corresponding continuation processes is depicted in Fig. 10a.

To shorten the presentation of the numerical calculations we only write down the explicit equations for the stable path, the equations for the unstable path immediately follow by reversing the time direction (see Rem. 2). We fix the time horizon $T = 500$ and note that the stable path consists of two arcs denoted as $(x_i, \lambda_i),\ i = 1, 2$. Therefore, we have to take into account the switching time (τ_1). The unknown parameter a also becomes a variable of the BVP, yielding

$$\dot{x}_1 = \tau_1 \left(x_1 \left(1 - \frac{x_1}{a} \right) - \frac{1}{0.625} \frac{x_1^2}{1 + x_1^2} \right) \tag{43a}$$

$$\dot{\lambda}_1 = \tau_1 \lambda_1 \left(-0.9 + \frac{2x_1}{a} + \frac{2x_1}{0.625(1 + x_1^2)^2} \right) \tag{43b}$$

$$\dot{x}_2 = (500 - \tau_1) \left(x_2 \left(1 - \frac{x_2}{a} \right) - \frac{1}{0.625} \frac{x_2^2}{1 + x_2^2} - \frac{x_2^2}{2} (1 - \lambda_2)^2 \right) \tag{43c}$$

$$\dot{\lambda}_2 = (500 - \tau_1) \lambda_2 \left(-0.9 + \frac{2x_2}{a} + \frac{2x_2}{0.625(1 + x_2^2)^2} - \frac{x_2}{2} (1 - \lambda_2) \right) \tag{43d}$$

$$x_1(0, a) = 2 \tag{43e}$$

$$x_1(1) = x_2(0), \quad \lambda_1(1) = \lambda_2(0) \tag{43f}$$

$$\frac{x_2(0)}{2} (1 - \lambda_2(0)) = 0 \tag{43g}$$

$$F_1(a)' \begin{pmatrix} \hat{x}_2(a) - x_2(1, a) \\ \hat{\lambda}_2(a) - \lambda_2(1, a) \end{pmatrix} = 0. \tag{43h}$$

An important and new property of this BVP is its explicit dependence on the parameter a. This affects the actual value of the equilibrium $(\hat{x}_2(a), \hat{\lambda}_2(a))$ and therefore the vector $F_1(a)$. In the following subsection about the general model a procedure is described how this problem can be solved.

Analogously to the stable path we solved the corresponding BVP for the unstable path which also consisted of two arcs. Therefore we set $T = -500$, denote the two arcs as $(x_i, \lambda_i),\ i = 3, 4$ and have to take into account the switching time (τ_2). Thus we find analogous equations to (43), which we will not repeat, with an equilibrium $(\hat{x}_4(a), \hat{\lambda}_4(a))$ and vector $F_2(a)$, also depending on the variable a.

Summing up we have eleven variables $(x_i, \lambda_i, \tau_j, a),\ i = 1, 2, 3, 4,\ j = 1, 2$ and ten equations, consisting of (43) and an analogous system for the unstable path. Thus one equation is missing, namely the defining property for a heteroclinic connection, saying that both paths start from the same initial point. Since the initial state is fixed at two, the missing equation concerns the initial costate,

which yields

$$\lambda_1(0) = \lambda_3(0). \tag{43i}$$

Solving the problem for the given values we find $a_b = 8.0218$ for the heteroclinic bifurcation parameter. The corresponding solution is depicted in Fig. 10b.

General model

To simplify the presentation we restrict the general case to one state models. But we consider a slight extension of the BVP, which allows for the computation of the bifurcation curve in a two parameter space $\mu = (\mu_1, \mu_2) \in \mathbb{R}^2$. The BVP in its general form becomes

$$\dot{y}_1(t,\mu) = T_1 f_1(y_1(t,\mu)), \mu),\ t \in [0,1] \tag{44a}$$
$$\dot{y}_2(t,\mu) = -T_2 f_2(y_2(t,\mu), \mu),\ t \in [0,1] \tag{44b}$$
$$F_1(\mu)'(y_1(1,\mu) - \hat{y}_1(\mu)) = 0,\ F_1(\mu) := \nu_1(\mu)^\perp \tag{44c}$$
$$F_2(\mu)'(y_2(1,\mu) - \hat{y}_2(\mu)) = 0,\ F_2(\mu) := \nu_2(\mu)^\perp \tag{44d}$$
$$y_1(0,\mu) = y_2(0,\mu) \tag{44e}$$
$$\varphi(y_1(\cdot,\mu), y_2(\cdot,\mu)) = 0 \tag{44f}$$
$$\Phi(y_1(\cdot,\mu), y_2(\cdot,\mu), \mu) = 0 \tag{44g}$$

additionally satisfying the algebraic equations

$$f_1(\hat{y}_1(\mu), \mu) = 0 \tag{44h}$$
$$f_2(\hat{y}_2(\mu), \mu) = 0 \tag{44i}$$

where $\nu_i(\mu)$ is the eigenvector corresponding to the negative eigenvalue of the Jacobian evaluated at $\hat{y}_i(\mu),\ i = 1, 2$.

We already noted in the previous fishery example, that the equilibria $\hat{y}_i(\mu)$ and therefore the vectors/matrices $F_i(\mu),\ i = 1, 2$ explicitly depend on the parameter values μ and may therefore change during the calculations. To handle such a situation different approaches are possible

- The equilibria $\hat{y}_1(\mu)$ and $\hat{y}_2(\mu)$ can be considered as additional variables satisfying the algebraic equations 44h–44i. Using an algorithm presented in Demmel et al. (12), Dieci and Eirola (13) the vectors (in general matrices) $F_i(\mu),\ i = 1, 2$ can then smoothly be continued.
- Due to the low dimensionality of the problem we solved 44h–44i within the solution finding of the boundary value solver, by solving the nonlinear equations 44h–44i and explicitly calculating the corresponding eigenvalues and eigenvectors. This is numerically time consuming but was efficient enough for the here presented model.

The first four equations 44a–44d describe the usual conditions for an unstable and stable path, with the extension of an explicit dependence on the parameter

value μ, as we already explained in detail. Equation (44e) states the crucial property of a heteroclinic connection, namely the coincidence of the stable and unstable manifold, and therefore the equality of the state and costate at time zero. Since this property is satisfied for any point of the heteroclinic connection Γ, there is an indeterminacy, which we remove by adding a further condition (44f), which specifies a unique point of Γ. The simplest possibility for such a function is by fixing the initial state at some specific value

$$\varphi(y_1(\cdot,\mu), y_2(\cdot,\mu)) := x_1^1(0) - \eta \tag{45a}$$

or

$$\varphi(y_1(\cdot,\mu), y_2(\cdot,\mu)) := \hat{x}_1^1(\mu)\gamma + \hat{x}_2^1(\mu)(1-\gamma), \quad \gamma \in (0,1). \tag{45b}$$

Equation (45b) fixes the initial state between the two equilibria, weighted by the constant γ. This has the advantage to (45a), that the initial state shifts if the equilibria change.

The last equation (44g) states a condition on the second parameter value. In its simplest form, if we are e.g. interested in the heteroclinic bifurcation for a fixed second parameter value, i.e., $\mu_2 = \mu_{20}$ this function simple becomes

$$\Phi(y_1(\cdot,\mu), y_2(\cdot,\mu), \mu) := \mu_2 - \mu_{20}. \tag{46}$$

Anyhow (46) provides also an easy way to calculate the bifurcation curve in the μ space, by setting at step k

$$\Phi := \mu_2 - \mu_2^{(k)} \quad \text{with} \quad \mu_2^{(k)} := \mu_2^{(0)} + k\Delta, \tag{47}$$

and some fixed step width $\Delta > 0$. For other functional forms see App. C.1.

Remark 7. For boundary value solver which can handle integral condition, (44f) is often formulated as an integral condition, which minimizes the L_1 norm between the previous and actual solution is also often used, but the conditions (45) are easy to implement and can particularly be used if the BVP solver cannot handle integral conditions. An extensive discussions of heteroclinic and homoclinic bifurcations the reader is referred to Homburg and Sandstede (19).

Heteroclinic bifurcation curve in the fishery model We now return to our previous example of the fishery model. In the first part of this section we solved the problem finding a heteroclinic bifurcation at (fixed) $p = 1$ and $a = 8.022$. To calculate the heteroclinic bifurcation curve in the interval $p \in [0.08, 1]$ at 200 points we used the continuation function

$$\Phi := p - \frac{0.92}{200}k, \;\; k = 1, \ldots, 200$$

and function

$$\varphi := x_1(0) - (\hat{x}_1(p^{(k)}) + \hat{x}_2(p^{(k)}))0.5,$$

for fixing the initial state of x.

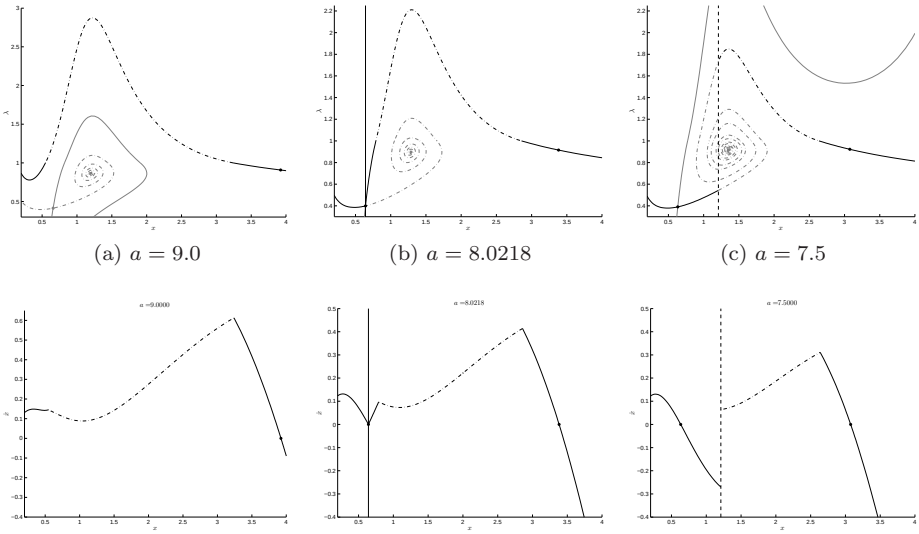

(a) $a = 9.0$ (b) $a = 8.0218$ (c) $a = 7.5$

(d) $a = 9.0$ (e) $a = 8.0218$ (f) $a = 7.5$

Figure 9: The case of an indifference attractor bifurcation is depicted for changing the parameter value a, (a,d) before, (b,e) at and (c,f) after the IAB. In the first row the paths in the state-costate are depicted and the second row shows the corresponding optimal vector field. The gray parts denote solutions satisfying the necessary optimality conditions, which are not optimal. Decreasing a the stable path of the optimal equilibrium comes closer to the unstable path until they coincide in a heteroclinic connection. This characterizes the indifference attractor bifurcation which lets emerge an indifference threshold shown by the dashed black line.

An analogous calculation, where the role of the equilibria are interchanged yield the lower branch of the heteroclinic bifurcation curve. In the bifurcation diagram Fig. 14a the heteroclinic bifurcation curves are depicted by black solid lines in. These two curves splits up the former region II (see App. A.4) into region IIa and region IIb. In both regions three equilibria of the canonical system exist. But in region IIb the optimal vector field consists of a globally stable equilibrium, whereas in region IIa two locally stable equilibria exist, having different regions of attraction. The bifurcation occurred at the heteroclinic bifurcation of the canonical system. The corresponding bifurcation of the optimal vector field is the so called indifference attractor bifurcation (IAB).

5.2 Indifference repeller bifurcation of type one (IRB1)

In the last section we analyzed the bifurcation, where the optimal vector field switched form a globally stable equilibrium to the case of two locally stable equilibria. Let us now have a closer look at the parameter space p-a for low

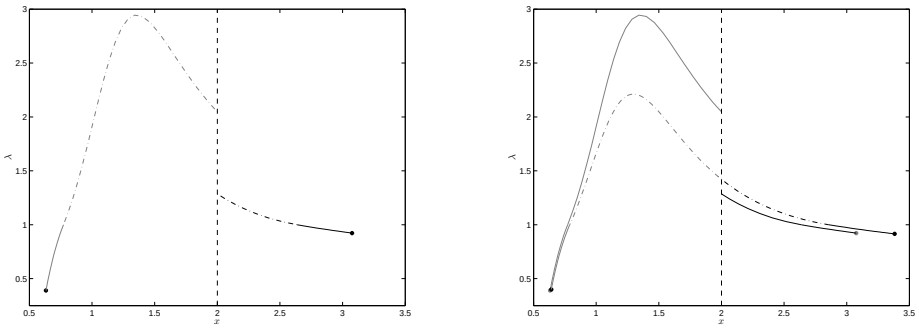

(a) $a = 7.5$ (b) $a = 8.0218$

Figure 10: This figure depicts the process of finding an indifference attractor bifurcation for the parameter value a. Therefore the unstable path (fine gray line) of the left equilibrium and the stable path (fine solid line) of the right equilibrium are continued to an initial state $x(0) = 2$ for $a = 7.5$. This is an approximation for the exact value a, where the heteroclinic connection occurs. Solving the BVP (44) determines the bifurcation parameter value as $a_b = 8.022$ and returns the heteroclinic connection between the two saddles (black dots). The gray line corresponds to the unstable path and the black line to the stable path.

values of p depicted in Fig. 14b and the blow up in Fig. 14c. The cross ($\times$) in region IIa correspond to the threshold case calculated in Sect. 4.2.3, and the plus (+) in region IIa correspond to the case with an indifference threshold near an unstable node (cf. Sect. 4.2.2). Thus for some intermediate value of a we expect a bifurcation of the optimal vector field from a system exhibiting two locally stable and one unstable equilibrium to a system with only two locally stable equilibria and a discontinuous vector field. Geometrically this bifurcation is driven from a change in the relative position of one of the stable paths and the strong unstable path[7] of the unstable node in the canonical system, cf. Fig. 12a-c. For a more detailed explanation the reader is referred to Kiseleva and Wagener (22) and Kiseleva (21), where this type of bifurcation is called an indifference repeller bifurcation of type one (IRB1).

At the bifurcation point the strong unstable path and stable path coincide. This property allows us to formulate the ascribing BVP in analogy to the heteroclinic connection, where the orthogonal vector to the unstable manifold is replace by the orthogonal vector to the strong unstable manifold. With this adaptation (44) also describes the IRB of type one.

[7]The unstable manifold corresponding to the maximum of the eigenvalues is called the strong unstable path.

IRB1 curve in the fishery model

We will not write down the explicit equations for the fishery model since these are clear from all the previous examples. For the actual computation we set $p = 0.03$ and let $a = 5.88$ be an approximation for the searched for bifurcation value. This yields three equilibria of the canonical system, where we took the lower saddle and unstable node for the calculations. The choice of the lower saddle was not arbitrary. Since the low equilibrium is the long run optimal solution for small a we can expect that, in the vicinity of $a = 5.88$, the bifurcation takes place between the low equilibrium and the unstable node.

For the unstable node the eigenvalues are $\xi_1 = 0.0183$ and $\xi_2 = 0.0817$ and the corresponding eigenvectors are given as

$$\nu_1 = \begin{pmatrix} -0.99999 \\ 0.005 \end{pmatrix} \quad \nu_2 = \begin{pmatrix} -0.9996 \\ 0.02797 \end{pmatrix}.$$

Thus ν_2 is the strong unstable eigenvector and its orthogonal complement yields the vector for the asymptotic boundary condition. The time horizons are chosen differently, namely $T_2 = 1000$ for the stable path and $T_1 = 200$ for the unstable path. Keeping $p = 0.03$ fixed and letting a be the free variable we find for the bifurcation value $a_b = 5.88825$. Continuation, as described in the previous Sect. 5.1, is used to find the curve of bifurcation values of IRB1 in the p-a space. The result is depicted by the (two) black dashed lines line in the bifurcation diagram Fig. 14b.

5.3 Indifference repeller bifurcation of type two (IRB2)

The bifurcation of the optimal vector field described before can also be driven by some other mechanism. Namely, by the transition from an unstable node to an unstable focus. In Kiseleva and Wagener (22) and Kiseleva (21) this bifurcation type is called an indifference repeller bifurcation of type two (IRB2).

In terms of the optimal vector field the two types of the IRB cannot be distinguished. But numerically the IRB2 reduces to the problem of finding an equilibrium $\hat{x}(\mu)$, for which the corresponding Jacobian $\hat{J}(\mu)$ satisfies

$$\operatorname{tr} \hat{J}(\mu) - 4 \det \hat{J}(\mu) = 0.$$

For the actual computations `MATCONT` was used to continue this system of equations and find the corresponding bifurcation curve (black dotted line in Fig. 14b).

5.4 Saddle-node bifurcation

The last codimension one bifurcation of the optimal vector field, which we have to mention is the saddle-node bifurcation. This bifurcation corresponds also to a saddle-node bifurcation in the canonical system. Numerically the saddle-node

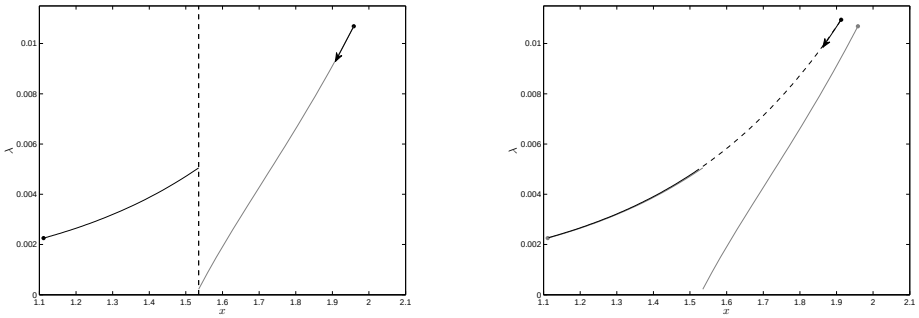

(a) $a = 5.88$ (b) $a = 5.888243$

Figure 11: This figure depicts the locating of an indifference repeller bifurcation for the parameter value a. (a) The strong unstable path (gray line) of the unstable node and the stable path (black line) of the lower saddle are continued to an initial state $x(0) = 1.8738$. (b) The fine lines and gray equilibria denote the approximated solution at $a_b = 5.88$. Solving the BVP (44) determines the bifurcation parameter value as $a_b = 5.8882$, where the strong unstable path and the stable path are connected. The vector points into the direction of the strong unstable eigenvector.

bifurcation reduces to the problem of finding an equilibrium $\hat{x}(\mu)$, for which the corresponding Jacobian $\hat{J}(\mu)$ is singular, i.e.

$$\det \hat{J}(\mu) = 0.$$

For the actual computations `MATCONT` was used to continue this system of equations and find the corresponding bifurcation curve (black dashed-dotted line in Fig. 14b).

5.5 Codimension two bifurcations (ISN) and (DIR)

In the following we denote bifurcation curves as essential if they are relevant for the optimal vector field and inessential if they are not relevant for the optimal vector field. Then we see that parts of the curves for the saddle-node bifurcation and the transition curve from the focus to the node are inessential (denoted by the gray dashed/dotted lines in Fig. 14b). The transition from the essential to the inessential parts of these bifurcation curves is described by bifurcations of codimension two, which roughly speaking means that two parameter values have to be determined for its detection. The numerical algorithms for their computations are described in this last section.

5.5.1 ISN bifurcation

When does the saddle-node curve become inessential? To answer this question we inspect the lower branch of the saddle-node curve of Fig. 14b in more

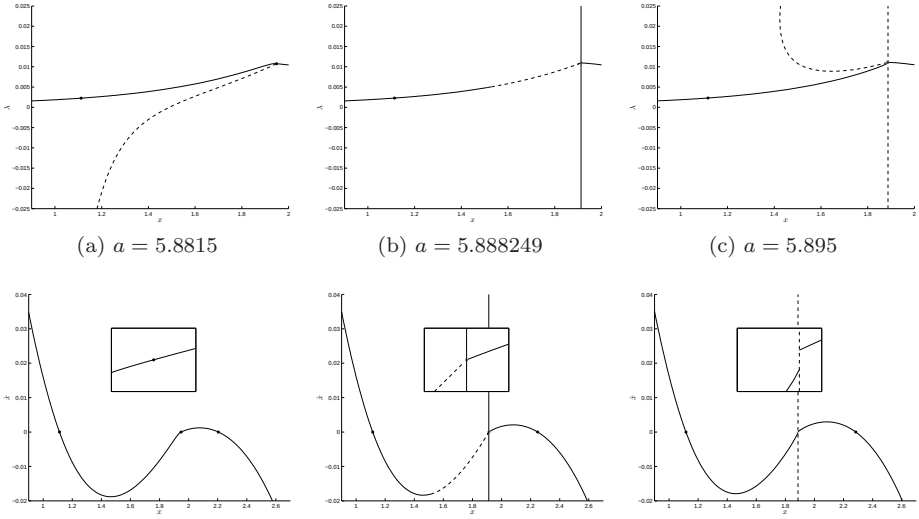

(a) $a = 5.8815$ (b) $a = 5.888249$ (c) $a = 5.895$

(d) $a = 5.8815$ (e) $a = 5.888249$ (f) $a = 5.895$

Figure 12: Solutions near an indifference repeller bifurcation of type one. In the first row the paths in the state-costate are depicted and in the second row the corresponding optimal vector field is shown, together with a blow-up of the region near the unstable node. Before the bifurcation (a,d) the strong unstable path (dashed line) lies below the stable path (solid line) and $\hat{x}_2$ is a threshold point with a continuous optimal vector field. At the bifurcation (b,e) the strong unstable and stable path coincide. After the bifurcation (c,f) the unstable node is replaced by an indifference threshold point and the optimal vector field becomes discontinuous.

detail. Therefore we calculate the solutions with parameter values lying on the essential and inessential part of the saddle-node curve (see Fig. 13a and Fig. 13c). The crucial difference is the relative position of the stable path (solid line) of the saddle point at the left and the unstable path (dashed line) of the non-hyperbolic equilibrium at the right. For the essential part the unstable path lies below the stable path. The corresponding optimal vector field reveals that for the essential part the right equilibrium is a semi-stable equilibrium, whereas in the inessential part there only exists one globally stable equilibrium (see Fig. 13d,e). Exactly at the bifurcation value the stable and unstable path coincide (see Fig. 13b,d). Thus this bifurcation point denoted as indifference saddle-node bifurcation (ISN) is the transition case from an indifference attractor bifurcation to an indifference repeller bifurcation of type one. This means that in a neighborhood of that bifurcation we find the IAB curve as well as the IRB curve and they touch the saddle-node curve exactly at the ISN bifurcation point. In Fig. 14b these points are denoted as black points. For a detailed description the reader is referred to Kiseleva (21).

For the numerical description we note that at the bifurcation point $\mu_b \in \mathbb{R}^2$ there exist two equilibria, a saddle $\hat{y}_1(\mu_b)$ and non-hyperbolic equilibrium $\hat{y}_2(\mu_b)$. These are connected via a heteroclinic connection path, given by the stable $y_1(\cdot, \mu_b)$ and unstable manifold path $y_2(\cdot, \mu_b)$. Denoting the Jacobian matrix of $\hat{y}_2(\mu)$ as $J_2(\mu)$ the corresponding BVP can be stated as

$$\dot{y}_1(t,\mu) = T_1 f_1(y_1(t,\mu)),\mu),\ t \in [0,1] \tag{48a}$$
$$\dot{y}_2(t,\mu) = -T_2 f_2(y_2(t,\mu),\mu),\ t \in [0,1] \tag{48b}$$
$$y_1^1(0,\mu) = y_2^1(0,\mu) \tag{48c}$$
$$\varphi(y_1(\cdot,\mu), y_2(\cdot,\mu)) = 0 \tag{48d}$$
$$F_1(\mu)'(y_1(1,\mu) - \hat{y}_1(\mu)) = 0,\ F_1(\mu) := \nu_s(\mu)^\perp \tag{48e}$$
$$F_2(\mu)'(y_2(1,\mu) - \hat{y}_2(\mu)) = 0,\ F_2(\mu) := \nu_u(\mu)^\perp \tag{48f}$$
$$\det(J_2(\hat{y}_2(\mu),\mu)) = 0. \tag{48g}$$

The boundary conditions 48a–48f are the analogs to that of the IAB (44), where $\nu_u(\mu)$ is the eigenvector corresponding to the positive eigenvalue. The last condition (48g) is the necessary condition for a saddle-node bifurcation.

5.5.2 DIR bifurcation

The second codimension two bifurcation denotes the switch from the essential parts of the transition curve from an unstable node to an unstable focus (see the dotted line in Fig. 14b). In Kiseleva and Wagener (22) this bifurcation is called the double indifference repeller bifurcation (DIR) and an exact definition is given in Kiseleva (21). The name reflects the fact that at this point the indifference repeller bifurcations of type one and two coincide. Analogous calculations to the previous example reveals that at the DIR bifurcation one of the unstable paths of the degenerate nodes coincides with the stable path of the saddle point. In

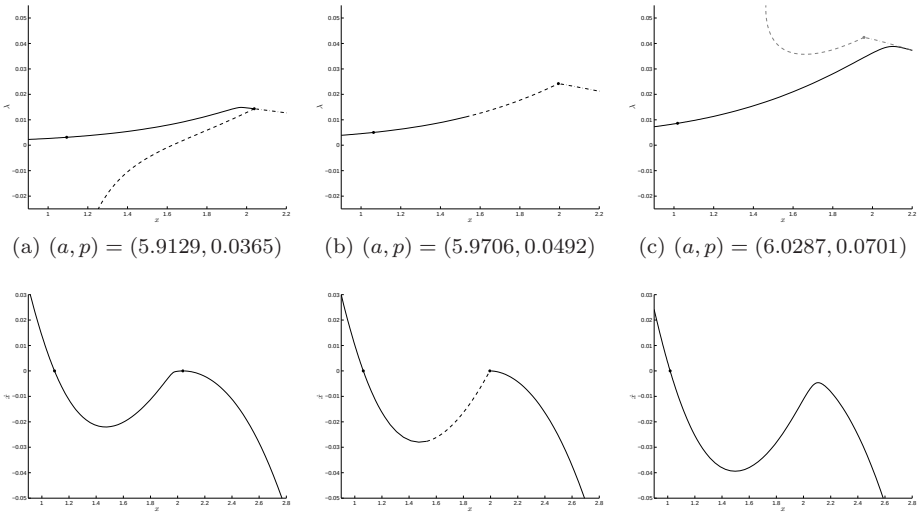

(a) $(a, p) = (5.9129, 0.0365)$ (b) $(a, p) = (5.9706, 0.0492)$ (c) $(a, p) = (6.0287, 0.0701)$

(d) $(a, p) = (5.9129, 0.0365)$ (e) $(a, p) = (5.9706, 0.0492)$ (f) $(a, p) = (6.0287, 0.0701)$

Figure 13: The situation near an ISN bifurcation is illustrated. The parameter values are chosen at the saddle-node bifurcation curve, yielding the equilibrium at the right $\hat{x}_2$ to be non-hyperbolic. In the first row the paths in the state-costate are depicted and in the second row the corresponding optimal vector field is shown. Before the bifurcation (a,d) the unstable path (dashed line) lies below the stable path (solid line). Right of $\hat{x}_2$ the optimal path is given by the center path (dashed-dotted line). The optimal vector field exhibits a locally stable and semi-stable equilibrium. At the bifurcation (b,e) the unstable path and the stable path coincide. After the bifurcation (c,f) the unstable and center path lie above the stable path. In the optimal vector field the lower equilibrium is now globally stable.

Fig. 14b the DIR bifurcation points are depicted as gray dots, which also finishes our bifurcation analysis of the fishery model in the p-a space.

Formally this bifurcation is characterized by the existence of a saddle and a degenerate node, where the stable path of the saddle coincides with one of the unstable paths of the degenerate node. Denoting the stable path as $y_1(\cdot, \mu)$, the unstable path as $y_2(\cdot, \mu)$ and the Jacobian matrix of the degenerate node as $J_2(\mu)$ with the corresponding eigenvectors $\nu_d(\mu),\ d = s, u$ the BVP for the DIR becomes

$$\dot{y}_1(t, \mu) = T_1 f(y_1(t, \mu), \mu),\ t \in [0, 1] \tag{49a}$$
$$\dot{y}_2(t, \mu) = -T_2 g(y_2(t, \mu), \mu),\ t \in [0, 1] \tag{49b}$$
$$y_1(0, \mu) = y_2(0, \mu) \tag{49c}$$
$$\varphi(y_1(\cdot, \mu), y_2(\cdot, \mu)) = 0 \tag{49d}$$
$$F_1'(y_1(1, \mu) - \hat{y}_1(\mu)) = 0,\ F_1 := \nu_s(\mu)^\perp \tag{49e}$$
$$F_2'(y_2(1, \mu) - \hat{y}_2(\mu)) = 0,\ F_2 := \nu_u(\mu)^\perp \tag{49f}$$
$$\operatorname{tr}(J_2(\mu)) - 4 \det(J_2(\mu)) = 0. \tag{49g}$$

The equations 49a–49f are the conditions characterizing the heteroclinic connection. The conditions for the two free parameter values are pinned down to the phase condition (49d) and (49g), which characterizes a degenerate node, i.e., an equilibrium in the transformation from an unstable focus to an unstable node.

Remark 8 (Non-uniqueness of the eigenvector). We note that for a degenerate node the eigenvalues are equal but the eigenspace is of dimension two, i.e., two linearly independent eigenvectors ν_1 and ν_2 exist. To determine the eigenvector ν_u we remind that the eigenvectors continuously depend on the parameter values. Let us therefore assume that we start with a solution exhibiting a strong unstable eigenvector $\nu_u^{(0)}$ near the actual bifurcation point. Then, by a continuity argument, the "correct" eigenvector ν_b is that which is nearest to the reference eigenvector $\nu_u^{(0)}$. We therefore choose the eigenvector maximizing the absolute value of the scalar product, i.e.,

$$|\nu_b' \nu_u^{(0)}| \geq |\nu_i' \nu_u^{(0)}|, \quad i = 1, 2.$$

6 Conclusion

An algorithm for the numerical analysis of the optimal vector field as it usually occurs in the context of economic and ecological applications was presented. These problems are often formulated as autonomous and nonlinear optimal control problems over an infinite time horizon, with only a few number of state and control variables. Even though the presentation was restricted to this class of problems these restrictions are no principal limitations of the algorithm. Anyhow, the number of state and control variables can be a severe restriction especially in the presence of various control constraints.

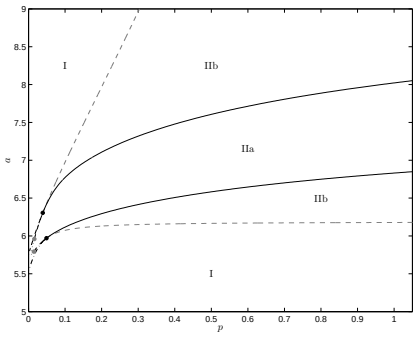

(a) Bifurcation diagram

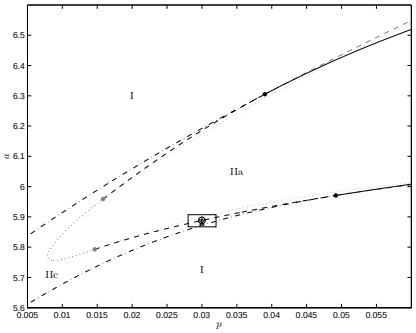

(b) Near $p = 0.03$

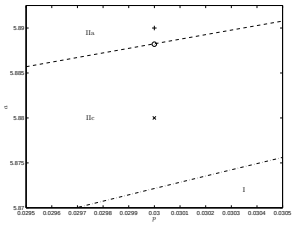

(c) Blow up

Figure 14: The bifurcation diagram of the optimal system in the p-a space is depicted (black lines) together with the bifurcation lines of the canonical system (gray lines). (a) gives an overall picture for the whole region of $p \in [0, 1]$. The bifurcation lines (solid line) separating region IIa and region IIb denote an IAB, cf. Sect. 5.1. In region IIa indifference thresholds exist, whereas in region I and region IIb the optimal solution is unique. In (b) the region for small values of p and appropriate values of a is illustrated in more detail. In region IIa a threshold point exists. The dashed black line denotes an IRB, cf. Sect. 5.2, of the second kind, whereas the dotted line denotes an IRB of the first kind. Bifurcations of codimension two are denoted by dots DIR (gray) and ISN, cf. Sect. 5.5, (black). Finally, (c) is a blow up of the region with the parameter values we used for the numerical examples, threshold point ($\times$), indifference threshold with unstable node ($+$) and IRB of the second kind ($\circ$).

In general indirect methods, applied to infinite time horizon problems, solve the finite time problem over a "large" time horizon. Under appropriate assumptions the finite time solution converges then to the infinite time horizon solution. Anyhow, for these methods the detection of multiple optimal solutions and bifurcation behavior of the optimal vector field can immediately become a challenging task. Differently, the here presented method does not solve a finite time horizon problem. In fact information about the long run behavior of the system is used, like convergence to an equilibrium, to derive appropriate boundary conditions at infinity. Not till that step these conditions are reformulated in a finite time setting.

What is crucial here is a careful examination of the possible behavior of the optimal vector field when time goes to infinity. This needs some further analysis aside from finding equilibria and stable paths of the canonical system. If states or control can go to infinity this has to be taken into account and may need an adaptation of the presented boundary conditions.

This approach may not be a good choice or even not applicable for large scale models, time critical applications, and of course by models which are not driven by ODEs. But for models with a small or moderate number of states/controls, with the focus on the analysis of the structural behavior of the system this approach is very useful.

To repeat the core idea underlying the here presented method. First the necessary conditions are derived. This yields the canonical system with its different ODEs for different combinations of binding and not binding (control) constraints. The dynamic structure of these ODEs can be analyzed to find equilibria and possible bifurcations. This first step yields insight into the dynamical variety and information about the equilibria (or, e.g. limit cycles) is then used to calculate paths converging to an equilibrium. The calculation of these paths is done by some continuation method and during this continuation regions can be detected where constraints become active or inactive. This is one of the problems indirect methods usually are confronted with, where this information has to be provided already before the calculation. In our approach the starting point is a solution (equilibrium, limit cycle) or at least a candidate, which is entirely known, and then successively extended into new regions.

Of course this strategy is time consuming but the process of continuation itself yields important information about the behavior of the optimal vector field. And having determined the solutions for a specific set of parameter values continuation can again be used to determine the solution paths for different parameter values.

And of course this method is not restricted to the class of models given by (1). Thus a further direction for future research work is an extension of this method to other types of models, including non-autonomous models with (non-)periodic dynamics, slow-fast systems, multi-stage systems, differential games, etc. Another important topic is the application to higher dimensional systems and their numerical (bifurcation) analysis. For these systems indifference and threshold manifolds exist, limit cycles can occur and possible bifurcations are numerous.

The core of the presented algorithms is the interplay between solving a BVP and continuation. At the moment the algorithm is implemented in a MATLAB package `OCMat` mainly written by the author.[8] In this package the native MATLAB boundary value solver are mainly used, which is not an ideal solution, since these solvers have no continuation method implemented. Therefore, the boundary value solver `BVPSUITE1.1` is tested and adapted.[9] This solver can handle singular problems, more general differential-algebraic equations and has integrated a continuation algorithm.

Anyhow, the author is also aware of `AUTO`, which is a powerful and widely used tool for continuation and BVPs. The pragmatic reason for using the solvers available for MATLAB is the integration in the package `OCMat`, where most of the necessary files for the numerical analysis are generated automatically and the problem can be formulated in an easy way. Additionally an interface is programmed for using `MATCONT` within `OCMat`. For a problem, like the full fishery model in three dimensions, the formulation of the problem and generation of the files for the numerical analysis only needs a few minutes. And after the file generation the numerical analysis can immediately start.

7 Acknowledgements

The work for this paper was financed in part by the Austrian Science Fund (FWF) under grant No. P 23084-N13 (A MATLAB Package for Analyzing Optimal Control Problems). I also appreciate the support by the Beijer Institute and the fruitful discussions with Anne-Sophie Crépin, Florian Wagener and Tatiana Kiseleva. Last I want to thank the reviewers for their constructive criticism who helped to improve the article substantially.

A General results for problem (9)

A.1 Proving that the fishery model is normal

Let us assume that $(x^*(\cdot), u^*(\cdot))$ is an optimal solution of the problem (9) and that $\lambda_0 = 0$.[10] Then, the Hamiltonian maximizing condition (12) reduces to

$$\max_{u \geq 0} \lambda(t) \left(x(t) \left(1 - \frac{x(t)}{a} \right) - \frac{1}{(c+\tau)} \frac{x(t)^2}{1+x(t)^2} - u x(t) \right). \tag{50}$$

We note that u only appears linearly in (50) yielding that the maximum depends on the sign of

$$\frac{\partial \mathcal{H}}{\partial u} = -\lambda(t) x(t). \tag{51}$$

[8] Download from `http://orcos.tuwien.ac.at/research/ocmat_software`.

[9] Download from `http://www.math.tuwien.ac.at/~ewa/download-bvp.php`.

[10] For infinite time horizon problems $\lambda_0 = 1$ is not guaranteed as is shown, e.g. in Halkin (17).

Since $x(t) > 0$ and $\lambda(t) \geq p > 0$ has to be satisfied by the non-negativity of Lagrangian multiplier, it follows that $u^*(t) = 0$. From the dynamics (9b) we therefore find that $x^*(\cdot)$ converges to a stable equilibrium $\hat{x} > 0$. Considering the utility function we see that in the neighborhood $B(\hat{x}, \varepsilon)$ of $\hat{x}$ we can choose a positive value of u on a finite time span ΔT such that

$$u(t)(px(t) - u(t)) > 0, \quad t \in [\tilde{T}, \tilde{T} + \Delta T]$$

yielding a positive objective value and therefore violating the optimality of $u^*(t) = 0$. This finally proves that λ_0 can be set to one.

A.2 Continuity of the optimal control and Lagrangian multiplier

For the Hamiltonian and Lagrangian

$$\begin{aligned}
&\mathcal{H}(x, u, \lambda) := \left(pux - u^2\right) + \lambda \left(x \left(1 - \frac{x}{a}\right) - \frac{1}{(c+\tau)} \frac{x^2}{1+x^2} - ux \right) \\
&\mathcal{L}(x, u, \lambda, \psi) := \mathcal{H}(x, u, \lambda) + \psi u \\
&k(u) := u \geq 0 \qquad \text{(52a)}
\end{aligned}$$

we find

$$\mathcal{L}_{uu}(x, u, \lambda, \psi) = -2 \qquad \text{(52b)}$$

$$k_u(u) = 1. \qquad \text{(52c)}$$

Thus, by (52b) the Lagrangian is strictly concave with respect to u and the control constraint (52a) satisfies the constraint qualification (52c).

At first the strict concavity of $\mathcal{L}$ implies the uniqueness of the optimal control value for a given state and costate. Furthermore, the continuity of the state and costate functions guarantee the existence of the left and right hand side limit of the control for every $t > 0$. Now let us assume that to the contrary the control is not continuous. Then there exists some $\tau > 0$ satisfying

$$u_1(\tau) := \lim_{t \to \tau^+} u(t) \neq \lim_{t \to \tau^-} u(t) =: u_2(\tau),$$

which yields a contradiction to the uniqueness of the control value.

The continuity of the control, the constraint qualification (52c) and the optimality condition

$$\mathcal{L}_u(x, u, \lambda, \psi) = 0 \Leftrightarrow \psi = -\mathcal{H}_u(x, u, \lambda)$$

yields that the Lagrangian multiplier $\psi(\cdot)$ is also continuous.

A.3 Existence and convergence of an optimal solution

In this section we prove Assumption 1 and Assumption 2 stated at the beginning. We start with the behavior of the solution for the time going to infinity.

Considering the total time derivative of the optimal control value in the interior of the control region (see (17)), i.e,

$$\dot{u}(t) = \frac{\mathrm{d}}{\mathrm{d}t}\left(\frac{x(t)}{2}(p - \lambda(t))\right).$$

Substituting the costate λ and the expressions for the dynamics finally yields

$$\begin{aligned}\dot{u}(t) = u(t)x(t)\left(\frac{1}{a} + \frac{1 - x(t)^2}{(c+\tau)(1-x(t)^2)^2) + \frac{1}{2}}\right) - u(t)^2 + ru(t) \\ - \frac{x(t)}{2}p\left(r - 1 + \frac{2x(t)}{a} + \frac{2x(t)}{(c+\tau)(1-x(t)^2)}\right). \quad (53)\end{aligned}$$

On the boundary of the control region the dynamics is trivially zero.

Summing up we find from the state dynamics (9b) and control dynamics (53) together with its extension on the boundary that there exist $x_m > 0$ and $u_m > 0$ such that the compact set $[0, x_m] \times [0, u_m]$ is invariant under the dynamics. Since limit cycles cannot occur for a positive discount rate $r > 0$, see e.g., Wagener (31), the Poincaré-Bendixson theorem assures that the paths converge to an equilibrium in the interior $\hat{x} > 0$ and $\hat{u} > 0$ or converge to an equilibrium at the boundary of the control region, i.e., $\hat{x} > 0$ and $\hat{u} = 0$. But repeating the arguments for the previous section we see that the latter case does not yield an optimal solution. Thus every optimal solution converges to an interior equilibrium. By the compactness of the region $[0, x_m] \times [0, u_m]$ the existence of an optimal solution is assured, which finally proved that Assumption 1 does hold. The constraint qualification (2), which reduces for $k(x, u) := u \geq 0$ to $k_u(x, u) = 1 > 0$ is trivially satisfied.

A.4 The canonical system and its bifurcations

Inspecting the canonical system

$$\dot{x}(t) = x(t)\left(1 - \frac{x(t)}{a}\right) - \frac{1}{(c+\tau)}\frac{x(t)^2}{1 + x(t)^2} - u^\circ(t)x(t) \quad (54a)$$

$$\dot{\lambda}(t) = \lambda(t)\left(r - 1 + \frac{2x(t)}{a} + \frac{2x(t)}{(c+\tau)(1+x(t)^2)^2}\right) - u^\circ(t) \quad (54b)$$

with

$$u^\circ(t) = \begin{cases} u^\bullet(t) & \text{for} \quad \lambda \geq p \\ 0 & \text{for} \quad \lambda \leq p \end{cases} \quad \text{and} \quad u^\bullet = \frac{x}{2}(p - \lambda), \quad (54c)$$

we immediately find that $x = \lambda = u^\circ = 0$ is always an equilibrium of the system. A simple argument shows that it is always better to keep x away from zero. Therefore, the zero equilibrium can be excluded and for the following analysis only positive equilibria have to be considered.

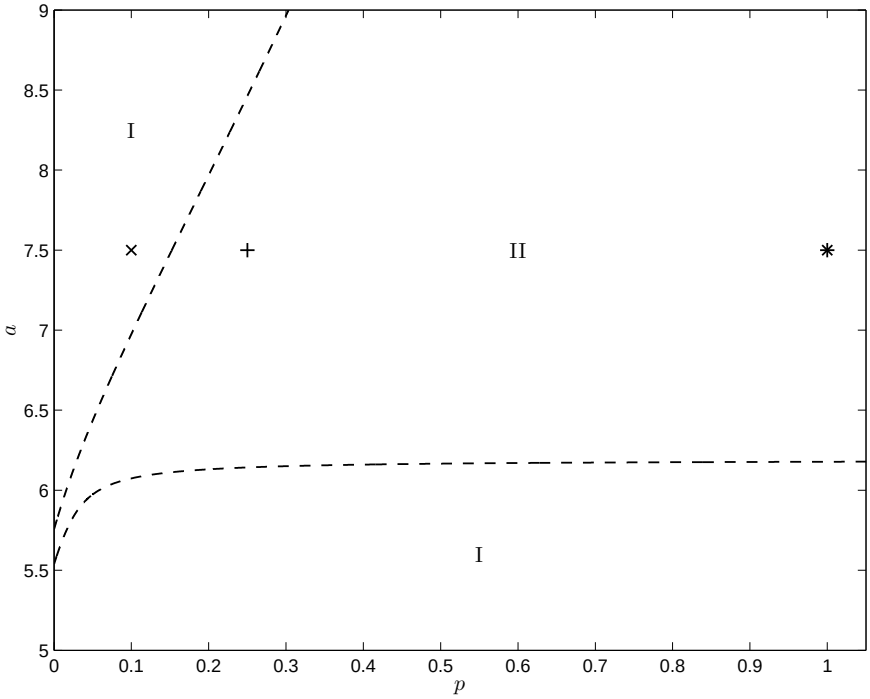

Figure 15: In the p-a parameter space the saddle-node bifurcation lines of the canonical system are depicted, separating the regions with one strictly positive equilibrium region (I) and three strictly positive equilibria region (II). Additionally the parameter values, which were used for the numerical examples of the optimal vector field, are shown, where $\times$ is analyzed in Sect. 4.1, $+$ in Sect. 4.2.1 and $*$ in Sect. 4.2.2.

As a simple starting point we consider the degenerated case with $p = 0$ and take the parameter values for r, τ and c are taken from the base case (cf. Tab. 1). Then the optimal control is identical zero $u \equiv 0$ and therefore non-zero equilibria have to satisfy the nonlinear equation

$$x\left(\frac{1}{a} + \frac{1}{(c+\tau)(1+x^2)}\right) = 1 \Leftrightarrow x^3 - ax^2 + x\left(1 + \frac{a}{c+\tau}\right) - a = 0, \qquad (55)$$

which exhibits at least one positive zero $\hat{x} > 0$. Since (55) reduces to a cubic equation we can even find the zeros analytically. Using Cardanos formula it can be shown that that for $a \in (5.7557, 5.5379)$ three (positive) roots of (55) exist and for $a \in (0, 5.7557) \cup (5.5379, \infty)$ only one root exists. Exactly at $a = 5.7557, 5.5379$ two of the three equilibria coincide which corresponds to a saddle-node bifurcation. These analytical results can be used to start a numerical continuation in p, e.g., by using `MATCONT`.

The result of the continuation in p is presented in Fig. 15, where the dashed

lines denote saddle-node bifurcations of the canonical system. Thus in the region I, a unique equilibrium exists, and in region II three equilibria can be found. For the optimal vector field we therefore expect in region I a globally stable equilibrium. To determine the equilibria of the optimal vector field for region II the stable paths with corresponding objective value have to be considered and is done in Sect. 4.

B Definitions and theorems for ODEs

B.1 Boundary value problems

Let $f : \mathbb{R}^n \to \mathbb{R}^n$ and $b : \mathbb{R}^n \times \mathbb{R}^n \to \mathbb{R}^n$ then a problem specified by

$$\dot{x}(t) = f(x(t)),\ t \in [0, T] \tag{56}$$
$$b(x(0), x(T)) = 0 \tag{57}$$

is called a (two-point) boundary value problem (TBVP or shortly BVP), and $b(x(0), x(T)) = 0$ are called the (two-point) boundary conditions. If (57) is replaced by a function $b : \mathbb{R}^n \times \ldots \times \mathbb{R}^n \to \mathbb{R}^n$ with

$$b(x(0), x(\tau_1), \ldots, x(\tau_m), x(T)) = 0, \quad 0 < \tau_1 < \ldots < \tau_m < T \tag{58}$$

problem (56) and (58) is called a multi-point boundary value problem (MBVP). Such MBVP can easily be transformed into a TBVP. As an example we present the transformation of an three-point problem, with

$$b(x(0), x(\tau), x(T)) = 0, \quad 0 < \tau < T. \tag{59}$$

First the ODE (56) is split into

$$\dot{x^1}(t) = f(x^1(t)),\ t \in [0, \tau]$$
$$\dot{x^2}(t) = f(x^2(t)),\ t \in [\tau, T].$$

Next the time transformations $t = s_1\tau$ and $t = \tau + s_2(T - \tau)$ yield

$$\dot{x^1}(s_1) = \tau f(x^1(s_1)),\ s_1 \in [0, 1]$$
$$\dot{x^2}(s_2) = (T - \tau) f(x^2(s_2)),\ s_2 \in [0, 1]$$

and the (59) becomes

$$b(x_1(0), x_1(1), x_2(1)) = 0.$$

Since the two arcs $x_1(\cdot)$ and $x_2(\cdot)$ are continuously connected the n boundary conditions

$$x_1(1) = x_2(0),$$

have to be added. As a drawback of this transformation the dimension of the problem is increased, and for the numerical computations both arcs are evaluated at the same time grid, which may numerically be costly too.

A standard text book for the numerical analysis of BVPs is Ascher et al. (1).

B.2 Stable manifold of an equilibrium

Let $\hat{x}$ be an equilibrium of the ODE (56) and ξ_i, $i = 1, \ldots, n$ be the eigenvalues of the Jacobian matrix $J(\hat{x})$. Then

$$\mathrm{E}^s = \mathrm{span}\{\nu_j \in \mathbb{R}^n : \mathrm{Re}(\xi_j) < 0\}, \quad \dim \mathrm{E}^s = n_- \tag{60}$$

is called the stable eigenspace.

Let $\hat{x}$ be an equilibrium of the ODE (56) and U be a neighborhood of $\hat{x}$; then the set

$$\mathrm{W}^s_{loc}(\hat{x}) = \{x \in U : x(0) = x, \lim_{t\to\infty} x(t) = \hat{x}, \text{and } x(t) \in U, t \geq 0\}$$

is called the *stable local manifold* of $\hat{x}$. The set

$$\mathrm{W}^s(\hat{x}) = \bigcup_{t\leq 0} \{x(t) : x(0) \in \mathrm{W}^s_{loc}(\hat{x})\} \tag{61}$$

is called the *global stable manifold* of $\hat{x}$. Reversing time gives the definition for the unstable case.

Now the following theorem can be proved:

Theorem 1 (Stable manifold theorem)**.** *Suppose that $\hat{x}$ is an equilibrium of (56), where $f \in C^k(\mathbb{R}^n)$. Let n_- be the corresponding dimensions of the stable subspaces E^s. Then there locally exist the local stable C^k manifold $\mathrm{W}^s_{loc}(\hat{x})$ of the dimensions n_- being tangent to E^s.*

A (hyperbolic) equilibrium $\hat{x}$ satisfying $0 < n_- < n$ is called a *saddle point* and a path converging to the saddle is called a *stable path* or *saddle path*.

Theorem 2 (Characterization of the stable eigenspace)**.** *Let $\hat{x}$ be a hyperbolic saddle of (56) with $n_- + n_+ = n$ and $n_- > 0$, $n_+ > 0$. Then $(x - \hat{x}) \in \mathrm{E}^s(\hat{x})$ if and only if $x - \hat{x}$ is orthogonal to every eigenvector b of the adjoint problem*

$$\dot{x}(t) = -\frac{\partial f}{\partial x}(\hat{x})' x(t),$$

where b corresponds to an eigenvalue ξ with $\mathrm{Re}\,\xi < 0$. Let $F = (b_1, \ldots, b_{n_+})$ consist of all eigenvectors of the adjoint problem with eigenvalues $\mathrm{Re}\,\xi_j < 0$, then

$$\mathrm{E}^s(\hat{x}) = \{x : F'(x - \hat{x}) = 0\}. \tag{62}$$

Remark 9. Alternatively to the characterization by the adjoint problem the real Schur decomposition (see 15, Ch. 7) can be used to determine F. This representation is advantageous for continuation problems where F changes (11, 13). For a MATLAB implementation which allows an ordering of the eigenvalues see Brandts (2).

C Numerical Continuation

We consider nonlinear (operator) equations of the form

$$F(x, \mu) = 0 \tag{63}$$

where $F : X \times \mathbb{R} \to Y$ is sufficiently smooth and X and Y are Banach-spaces, and a pair (x, μ) satisfying (63) is called a *solution of (63)*.[11] An important example for such a nonlinear operator equation is the BVP (56)-(57).

The task of *continuation* (*path-following*) is now, given a specific solution (x_s, μ_s), find a (smooth) solution curve $x(\mu)$ satisfying

$$F(x(\mu), \mu) = 0$$

with $\mu \in [\mu_s, \mu_e]$.

The existence of such a solution curve $x(\mu)$ is, e.g., assured by the implicit function theorem, existence theorems under less restrictive conditions can be found in Dontchev and Rockafellar (14). For continuation in context with ODEs and BVPs the reader is referred to Kuznetsov (26), Winkler (33), Kitzhofer et al. (23) and Krauskopf et al. (24).

The numerical task of a *continuation process* is to provide an algorithm allowing the successive computation of points $x(\mu_i)$, $i = 1, \ldots, N$, approximating the solution curve $x(\mu)$ with $\mu_N = \mu_e$.

C.1 Continuation Algorithms

Next we present two simple continuation algorithms working "above" some zero finding solver, in our context BVP solver (for a more detailed description see, e.g., 16). This approach has the advantage of being independent on the actually used solver, but the disadvantage of disregarding structural information of the specific solver. Anyhow, even for the "above" method a more sophisticated continuation algorithm can be implemented, cf. Winkler (33), but the following proved sufficient for all problems we analyzed so far.

The problem we are facing is

$$F(x, \mu) = 0, \tag{64}$$

with $F : C^1 \times \mathbb{R}^p \to C^0$ a BVP, depending on the parameter value(s) μ. Then a given solution (x_s, μ_s) shall be continued to some $\mu_e \neq \mu_s$.

Reparameterization: We reparameterize the problem by introducing a scalar continuation variable $\gamma \in [0, 1]$ setting

$$\begin{aligned} \mu(\gamma) &:= \mu_s + \gamma(\mu_e - \mu_s) \\ &= \mu_s(1 - \gamma) + \gamma\mu_e, \ \gamma \in [0, 1], \end{aligned} \tag{65}$$

with $\mu(0) = \mu_s$ and $\mu(1) = \mu_e$.

[11] A reader unfamiliar with functional analysis can replace Banach-spaces by Euclidean spaces. In fact since for numerical purposes infinite dimensional spaces are discretized, the actual computation takes place in Euclidean spaces.

Initialization: We define some positive constant $0 < \sigma_0 < 1$ and determine the solution of (63) for

$$\gamma_1 = \gamma_0 + \sigma_0, \tag{66}$$

with $x_0 = x_s$ and $\gamma_0 = 0$.

Continuation Step $i > 1$: To follow solutions, where the stable manifold exhibits turning points we augment problem (64) by adding

$$\Phi(\gamma, \gamma_i, \sigma) = \gamma - \gamma_i - \sigma \tag{67}$$

$$\Phi(x, \gamma, x_i, \gamma_i, \sigma) := \|x - x_i\|^2 + (\gamma - \gamma_i)^2 - \sigma^2, \tag{68}$$

$$\Phi(x, \gamma, x_i, x_{i-1}, \gamma_i, \gamma_{i-1}, \sigma) := \begin{pmatrix} \Delta x_i \\ \Delta \gamma_i \end{pmatrix}' \begin{pmatrix} x - x_i \\ \gamma - \gamma_i \end{pmatrix} - \sigma \left\| \begin{pmatrix} \Delta x_i \\ \Delta \gamma_i \end{pmatrix} \right\|^2, \tag{69}$$

$$\Delta x_i = x_i - x_{i-1},\ \Delta \gamma_i = \gamma_i - \gamma_{i-1},$$

where $x_k = x(\gamma_k)$, $k = i-1, i$ are previously detected solutions and $\sigma > 0$ is a given constant, assuring that the new solution differs from the previous solution. Geometrically (68) describes a circle of radius σ around the solution at step i, whereas (69) ascribes a line perpendicular to the direction of the linear extrapolation of the last two detected solutions.

Prediction Step: The approximated solution is linearly extrapolated from the two previous solutions, (x_{i-1}, γ_{i-1}) and (x_i, γ_i), yielding

$$\tilde{x}_{i+1} = x_i + \alpha\,(x_i - x_{i-1}) = x_i(\alpha + 1) - \alpha x_{i-1} \tag{70a}$$

$$\tilde{\gamma}_{i+1} = \gamma_i + (\gamma_i - \gamma_{i-1}) = \gamma_i(\alpha + 1) - \alpha \gamma_{i-1}. \tag{70b}$$

The constant α is determined, depending on the current and previous step size given by the ratio

$$\alpha = \frac{\sigma_{i+1}}{\sigma_i}.$$

References

[1] U.M. Ascher, R.M.M. Mattheij, and R.D. Russell. *Numerical Solution of Boundary Value Problems for Ordinary Differential Equations*. Society for Industrial and Applied Mathematics, Philadelphia, PA, 1995.

[2] J.H. Brandts. Matlab code for sorting real Schur forms. *Numerical Linear Algebra with Applications*, 9(3):249–261, 2002.

[3] J.P. Caulkins, G. Feichtinger, D. Grass, M. Johnson, G. Tragler, and Y. Yegorov. Placing the poor while keeping the rich in their place: Separating strategies for optimally managing residential mobility and assimilation. *Demographic Research*, 13(1):1–34, 2005.

[4] J.P. Caulkins, G. Feichtinger, D. Grass, and G. Tragler. A model of moderation: Finding Skiba points on a slippery slope. *Central European Journal of Operations Research*, 45–64(1):13, 2005.

[5] J.P. Caulkins, G. Feichtinger, D. Grass, and G. Tragler. Bifurcating DNS thresholds in a model of organizational bridge building. *Journal of Optimization Theory and Applications*, 133(1):19–35, 2007.

[6] J.P. Caulkins, D. Grass, G. Feichtinger, and G. Tragler. Optimizing counter-terror operations: Should one fight fire with "fire" or "water"? *Computers and Operations Research*, 35(6):1874–1885, 2008.

[7] J.P. Caulkins, G. Feichtinger, D. Grass, and G. Tragler. Optimal control of terrorism and global reputation: A case study with novel threshold behavior. *Operations Research Letters*, 37(6):387–391, 2009.

[8] J.P. Caulkins, G. Feichtinger, D. Grass, R.F. Hartl, and P.M. Kort. Two state capital accumulation with heterogeneous products: disruptive vs. non-disruptive goods. *Journal of EconomicDynamics and Control*, 35(4): 462–478, 2011.

[9] A.-S. Crépin. Using fast and slow processes to manage resources with thresholds. *Environmental and Resource Economics*, 36(2):191–213, 2007.

[10] F.R. de Hoog and R. Weiss. An approximation theory for boundary value problems on infinite intervals. *Computing*, 24(2-3):227–239, 1980.

[11] J. Demmel. Three methods for refining estimates of invariant subspaces. *Computing*, 38(1):43–57, 1987.

[12] J.W. Demmel, L. Dieci, and M.J. Friedman. Computing connecting orbits via an improved algorithm for continuing invariant subspaces. *SIAM Journal on Scientific Computing*, 22(1):81–94, 2000.

[13] L. Dieci and T. Eirola. On smooth decompositions of matrices. *SIAM Journal on Matrix Analysis and Applications*, 20(3):800–819, 1999.

[14] A.S. Dontchev and R.T. Rockafellar. *Implicit Functions and Solution Mappings: A View from Variational Analysis*. Springer Verlag, 2009.

[15] G. Golub and C. van Loan. *Matrix Computations*. The Johns Hopkins University Press, Baltimore, 3rd edition, 1996.

[16] D. Grass, J.P. Caulkins, G. Feichtinger, G. Tragler, and D.A. Behrens. *Optimal Control of Nonlinear Processes: With Applications in Drugs, Corruption, and Terror*. Springer Verlag, Berlin, 2008.

[17] H. Halkin. Necessary conditions for optimal control problems with infinite horizons. *Econometrica*, 42(2):267–272, March 1974.

[18] R.F. Hartl. A simple proof of the monotonicity of the state trajectories in autonomous control problems. *Journal of Economic Theory*, 40(1):211–215, 1987.

[19] A.J. Homburg and B. Sandstede. Homoclinic and heteroclinic bifurcations in vector fields. In *Handbook of Dynamical Systems*, volume 3, pages 379–524. Elsevier Science, 2010. doi: DOI:10.1016/S1874-575X(10)00316-4. URL http://www.sciencedirect.com/science/article/B8JCJ-51378BK-D/2/2fefddf72e8b6886ba323

[20] M.I. Kamien and N.L. Schwartz. *Dynamic Optimization: The Calculus of Variations and Optimal Control in Economics and Management*. North-Holland, Amsterdam, 2nd edition, 1991.

[21] T. Kiseleva. *Structural Analysis of Complex Ecological Economic Optimal Control Problems*. PhD thesis, University of Amsterdam, Center for Nonlinear Dynamics in Economics and Finance (CeNDEF), 2011.

[22] T. Kiseleva and F.O.O. Wagener. Bifurcations of optimal vector fields in the shallow lake system. *Journal of Economic Dynamics and Control*, 34 (5):825–843, 2010.

[23] G. Kitzhofer, O. Koch, and E. Weinmüller. Pathfollowing for essentially singular boundary value problems with application to the complex Ginzburg-Landau equation. *BIT Numerical Mathematics*, 49(1):141–160, 2009.

[24] B. Krauskopf, H.M. Osinga, and J. Galán-Vioque, editors. *Numerical Continuation Methods for Dynamical Systems: Path following and boundary value problems*. Springer Verlag, Dordrecht, 2007.

[25] P. Kunkel and O. von dem Hagen. Numerical solution of infinite-horizon optimal-control problems. *Computational Economics*, 16(3):189–205, 2000.

[26] Y.A. Kuznetsov. *Elements of Applied Bifurcation Theory*. Springer Verlag, New York, 2nd edition, 1998.

[27] A. Levy, F. Neri, and D. Grass. Macroeconomic aspects of substance abuse: Diffusion, productivity and optimal control. *Macroeconomic Dynamics*, 10 (2):145–16, 2006.

[28] P. Michel. On the transversality condition in infinite horizon optimal problems. *Econometrica*, 50(4):975–985, 1982.

[29] K.J. Palmer. Exponential dichotomies and transversal homoclinic points. *Journal of Differential Equations*, 55(2):225–256, 1984.

[30] A. Seierstad and K. Sydsaeter. *Optimal Control Theory with Economic Applications*. North-Holland, Amsterdam, 1986.

[31] F.O.O. Wagener. Skiba points and heteroclinic bifurcations, with applications to the shallow lake system. *Journal of Economic Dynamics and Control*, 27(9):1533–1561, 2003.

[32] F.O.O. Wagener. Skiba points for small discount rates. *Journal of Optimization Theory and Applications*, 128(2):261–277, 2006.

[33] R. Winkler. Path-following for two-point boundary value problems. Seminarbericht 78, Department of Mathematics, Humboldt-University Berlin, Germany, 1985.

[34] I. Zeiler, J.P. Caulkins, D. Grass, and G. Tragler. Keeping options open: an optimal control model with trajectories that reach a DNSS point in positive time. *SIAM Journal on Control and Optimization*, 48(6):3698–3707, 2010.